

TOPICAL REVIEW

Collisionless magnetic reconnection in the magnetosphere

To cite this article: Quanming Lu *et al* 2022 *Chinese Phys. B* **31** 089401

View the [article online](#) for updates and enhancements.

You may also like

- [ELECTRON ACCELERATION BY MULTI-ISLAND COALESCENCE](#)
M. Oka, T.-D. Phan, S. Krucker et al.
- [Energy Partition between Ion and Electron of Collisionless Magnetic Reconnection](#)
Masahiro Hoshino
- [Electron-only Reconnection in an Ion-scale Current Sheet at the Magnetopause](#)
S. Y. Huang, Q. Y. Xiong, L. F. Song et al.

Collisionless magnetic reconnection in the magnetosphere

Quanming Lu(陆全明)^{1,2,†}, Huishan Fu(符慧山)^{3,4}, Rongsheng Wang(王荣生)^{1,2}, and San Lu(卢三)^{1,2}

¹CAS Key Laboratory of Geospace Environment, School of Earth and Space Sciences, University of Science and Technology of China, Hefei 230026, China

²CAS Center for Excellence in Comparative Planetology, Hefei 230026, China

³School of Space and Environment, Beihang University, Beijing 100191, China

⁴Key Laboratory of Space Environment Monitoring and Information Processing, Ministry of Industry and Information Technology, Beijing 100191, China

(Received 18 April 2022; revised manuscript received 3 June 2022; accepted manuscript online 8 June 2022)

Magnetic reconnection underlies the physical mechanism of explosive phenomena in the solar atmosphere and planetary magnetospheres, where plasma is usually collisionless. In the standard model of collisionless magnetic reconnection, the diffusion region consists of two substructures: an electron diffusion region is embedded in an ion diffusion region, in which their scales are based on the electron and ion inertial lengths. In the ion diffusion region, ions are unfrozen in the magnetic fields while electrons are magnetized. The resulted Hall effect from the different motions between ions and electrons leads to the production of the in-plane currents, and then generates the quadrupolar structure of out-of-plane magnetic field. In the electron diffusion region, even electrons become unfrozen in the magnetic fields, and the reconnection electric field is contributed by the off-diagonal electron pressure terms in the generalized Ohm's law. The reconnection rate is insensitive to the specific mechanism to break the frozen-in condition, and is on the order of 0.1. In recent years, the launching of Cluster, THEMIS, MMS, and other spacecraft has provided us opportunities to study collisionless magnetic reconnection in the Earth's magnetosphere, and to verify and extend more insights on the standard model of collisionless magnetic reconnection. In this paper, we will review what we have learned beyond the standard model with the help of observations from these spacecraft as well as kinetic simulations.

Keywords: collisionless magnetic reconnection, magnetosphere

PACS: 94.05.–a, 94.30.cp, 94.30.–d

DOI: 10.1088/1674-1056/ac76ab

1. Introduction

Magnetic reconnection, accompanying with the topological change of magnetic field lines, provides a physical mechanism to transfer magnetic energy into plasma kinetic energy, leading to ion and electron heating, and particle acceleration to high energies.^[1–6] It underlies many explosive phenomena across a wide range of natural and laboratory plasmas, whose source of energy comes from the magnetic field. These explosive phenomena include solar flare,^[7,8] substorm in the Earth's magnetospheres,^[9,10] and sawtooth oscillations in tokamaks.^[11] The first physical model for magnetic reconnection was proposed by Sweet and Parker separately, which is based on magnetohydrodynamics (MHD) and named as the Sweet–Parker model.^[12,13] In this model, the magnetic fields at the two sides of current sheet have the reverse direction, and the plasma in the upstream, which is frozen in the magnetic fields, move toward the current sheet. In the current sheet, a reconnection electric field perpendicular to the reconnection plane is induced in a region where the plasma is unfrozen in the magnetic field. The region is called as the diffusion region, where the plasma is accelerated and then leaves away in the outflow direction. The dissipation of magnetic energy occurs in the diffusion region through the Ohm's heating, which depends on the resistance. Because the plasma in space envi-

ronment usually has a small density and high temperature, the collision among the particles can be negligible, and the plasma is collisionless. The resistance in such a kind of plasma is very small, therefore, the conversion rate from magnetic energy to plasma kinetic energy is too small to account for the explosive phenomena in space environment.

To overcome the slow conversion rate in the Sweet–Parker model, a collisionless magnetic reconnection model is proposed. In this model, the diffusion region has two substructures: the ion and electron diffusion region, and the electron diffusion region is embedded in the ion diffusion region.^[2,14,15] Figure 1 shows the substructures of the diffusion region in collisionless magnetic reconnection. In the ion diffusion region with the scale size at the ion inertial length, the electrons are magnetized and move toward the X line along the magnetic field lines in the separatrix region, while the ions are demagnetized.^[16,17] In the electron diffusion region with the scale size at the electron inertial length, the electron motions also become demagnetized, which leads to the nongyrotropic electron distribution, and the reconnection electric field is supported primarily by the off-diagonal electron pressure term in the generalized Ohm's law.^[16,18–22] The electrons are accelerated in the electron diffusion region by the reconnection electric field, and then directed away along the magnetic field below the inflow electrons in the ion diffusion

[†]Corresponding author. E-mail: qmlu@ustc.edu.cn

region.^[17,23,24] The electron flow in the reconnection plane constitutes the Hall current, which produces a quadrupolar structure of the out-of-plane magnetic field in the ion diffusion region.^[17,25–29] The conversion rate from magnetic energy to plasma kinetic energy in collisionless magnetic reconnection is sufficiently fast to account for explosive phenomena in space environment.

Magnetic reconnection may occur in the Earth’s magnetosheath, magnetopause and magnetotail. When the interplanetary magnetic field (IMF) has a southward component, magnetic reconnection may occur in the magnetopause, and then magnetic and plasma energy can enter the magnetosphere, which at last trigger magnetic reconnection in the magnetotail.^[30,31] Magnetic reconnection may also occur in the magnetosheath, which usually exists in a turbulent state.^[32,33] In these regions, the ion inertial length is hundreds of kilometers, while the electron inertial length is only tens of kilometers. Recently, the launching of Cluster, the Time History of Events and Macroscale Interactions during Substorms (THEMIS), Magnetospheric Multiscale (MMS) and other satellites have provided opportunities to study magnetic reconnection in the Earth’s magnetosphere with high-resolution plasma measurements. Cluster is a four-satellite tetrahedral constellation operated by European Space Agency (ESA), and was delivered in the summer of 2000.^[34] The inter-spacecraft distance can be reduced to only several hundreds of kilometers, which has offered a chance to study the ion diffusion region. The THEMIS mission was launched by NASA on February 17, 2007, and it consists of five identical satellites.^[35] These five satellites can line up along the Earth’s magnetotail to track the motion of particles, plasma, and waves from one to another, thus they are suitable to investigate the occurring of magnetotail reconnection and the consequent effects, like dipolarization fronts. MMS is an NASA four-spacecraft constellation mission launched on March 12, 2015.^[36] Because it can provide observational data with high spatial resolution (~ 10 -km interspacecraft separation) and unprecedented time scales (30 ms for 3D electron distribution functions), the kinetic processes occurring in the electron diffusion region have been resolved. In this paper, we will focus on the recent progresses on collisionless magnetic reconnection in the magnetotail, magnetopause and magnetosheath based on *in-situ* observations from these satellites as well as kinetic simulations, and describe the new physics beyond the standard model of collisionless magnetic reconnection.

2. Magnetic reconnection in the magnetotail

Magnetic reconnection in the magnetotail usually occurs around $X_{GSM} = -20R_E$ (where R_E is the Earth’s radius, and GSM denotes the geocentric solar magnetospheric coordinates, which is a widely-used coordinate system in space

plasma physics). Because the plasma and magnetic field on both sides of the plasma sheet are nearly identical except for the direction of magnetic field, magnetic reconnection in the magnetotail is generally believed to be symmetric. In addition, magnetic reconnection is generally an unsteady process. Besides the diffusion region, magnetic reconnection can also produces transient structures in the downstream. Here, we will describe the structures and physical processes in the diffusion region and downstream, respectively.

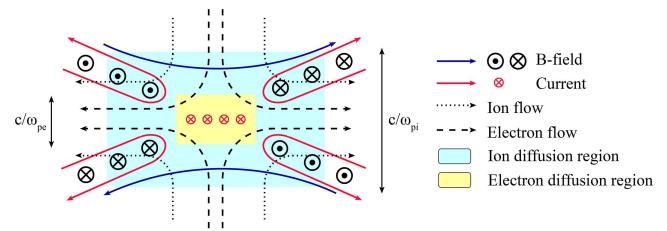


Fig. 1. The substructures of the diffusion region in collisionless reconnection.

2.1. Structures and physical processes in the diffusion region

The solar wind sweeps the Earth’s magnetic field into a huge tail, named magnetotail, as shown in Fig. 2. The size of the Earth’s magnetotail is controlled by the solar wind condition and the Earth’s intrinsic magnetic field. It will be stretched tightly and extend hundreds of the Earth radii from the Earth due to the solar wind dynamical pressure. Disruptions in the magnetotail create the colorful and bright auroras in the polar region and intensify the electric current surrounding the Earth, resulting in the substorm and/or magnetic storm.^[10,37–41] Up to date, magnetic reconnection in the near-Earth magnetotail is well known to be the main driver for the substorm.^[9,42] Thanks to a few spacecraft missions, *e.g.*, Cluster, THEMIS, MMS, and so on, a big progress has been achieved last twenty years. Based on the theory and numerical simulations, the key region for the occurrence of magnetic reconnection is the diffusion region.^[43] In the diffusion region, the ion and electron would decouple from the magnetic field line in their individual diffusion region and magnetic free energy is explosively released. Before the observation of the reconnection diffusion region, the earthward bursty bulk flows are extensively observed and regarded as the remarkable feature of the reconnection.^[44–47]

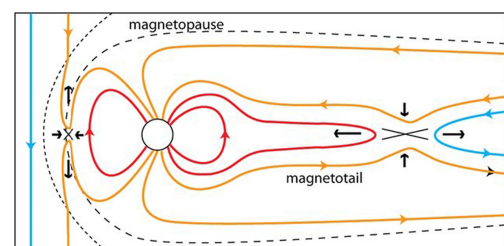


Fig. 2. A schematic illustration for the Earth’s magnetosphere.

In the magnetotail, the ion diffusion was firstly in situ detected by Øiersøst *et al.*^[48] with the Wind data. In this event, the spacecraft crossed the reconnection diffusion region from one outflow to the other according to the ion flow reversal from earthward to tailward, and observed the sign change of the out-of-plane magnetic field component. This is consistent with the quadrupolar magnetic field structure surrounding the X-line.^[14,36,49] Additionally, a low-energy electron beam was measured in the separatrix region, namely so-called Hall electron inflow. The observations provided the first *in situ* evidence in the magnetotail for the Hall effect, which was thought to be the key for the fast reconnection at that time. During the same reconnection event, the electrons were significantly heated inside the diffusion region and energetic electrons were detected therein as well. The energy of the accelerated electron reached as high as 200 keV. It means that the electrons can be accelerated directly to relativistic energy.^[50] On the contrary, ions were heated as well but there was no high-energy ion detected there. Shortly, a series of papers studied the ion and electron flow properties in the vicinity of the ion diffusion region based on the Geotail and Cluster missions.^[24,39,51–53] It is found that the low-energy electron inflowing beam was always detected at the outer boundary of the Hall magnetic field region. The width of the Hall magnetic field was a few ion inertial lengths. However, it extends as far as tens of ion inertial lengths along the outflow direction.

Based on the measurements onboard Geotail and Cluster in the magnetotail, the electron flow feature inside the ion diffusion region was investigated in detail. In the separatrix regions, the electrons mainly show the beam-like distribution and were injected into the X-line region.^[52,54] In the vicinity of the X line, the electrons display field-aligned bidirectional distribution at lower energies and become isotropic at higher energies. This kind of electron distribution was primarily attributed to the magnetic mirror and electrostatic potential around the X-line region.^[55–58] In the outflow region, at the edge of the outflow region there is a high-speed electron stream directed away from the X line. These electrons are accelerated in the X-line region and then ejected away from therein.

Electron density cavity is another striking feature in the separatrix region during magnetic reconnection.^[59–61] In general, the low-energy inflowing electrons are collocated with the density cavity. Even though the cavity can extend very far along the separatrices, its width is very narrow, only about a few electron inertial lengths. Inside the cavity, the intense electrostatic fluctuations are very common.^[62–64] The electron phase space hole and double layers are frequently observed in the separatrix region.^[58,59] Thus, the electrons may be accelerated by the electrostatic structures, even up to hundreds of keV in the separatrix region.

A guide field associated with magnetotail reconnection is generally detected although it is weak or moderate in most situations.^[60,64] Then, the reconnection diffusion region would be altered by the guide field. The simulations suggested that the guide field can dramatically affect the particle dynamics and the structure of the Hall electric field as well as Hall magnetic field in the ion diffusion region,^[65,66] although it does not alter the reconnection rate and the in-plane magnetic field very much. The distorted Hall magnetic field and electric field was indeed observed inside the ion diffusion region. Because of the addition of the guide field, the outflow electron current was deflected by the Lorentz force to one side of the current sheet, resulting in the distortion of the Hall electric and magnetic field structures.

Magnetic flux ropes are frequently detected in the process of magnetotail magnetic reconnection.^[60,67,68] The typical signature of magnetic flux rope consists of a bipolar variation of magnetic field component in the normal direction of the plasma sheet and the peak of magnetic field component in the dawn-dusk direction during the bipolar variation. Thus, the flux rope is supposed to be a helical magnetic structure. Magnetic reconnection occurs simultaneously at multiple points and then the flux rope would be created between any two adjacent magnetic reconnection sites.^[69] There exists another potential formation mechanism of magnetic flux rope. The electron current layer extends very long during reconnection and then breaks down into a series of small-scale current layers which are the flux ropes.^[70,71] Magnetic flux ropes have been detected inside the diffusion region as well,^[72,73] which supports the second mechanism as mentioned above.

Magnetic flux ropes play a key role during magnetic reconnection. The electron current layer, *i.e.*, the electron diffusion region, shortened once magnetic flux rope is generated, which raises the reconnection rate sharply.^[70–72] The electrons can be directly accelerated to hundreds of keV inside the flux ropes.^[75–77] The acceleration mechanism(s) is still controversial. The induced electric field inside flux ropes can be very important for the electron acceleration.^[78–81] The electrons can be accelerated via Fermi acceleration inside the contracting magnetic flux rope.^[23,82] In addition, various plasma waves can be excited inside the flux ropes,^[83] including the whistler waves, lower-hybrid drift waves, and electrostatic waves. These waves can energize the electrons as well inside the flux rope. As the flux rope propagates inside the plasma sheet, the magnetic field fluxes are accumulated in the trailing part and the electrons can be efficiently energized by betatron there.^[84] In addition, the secondary reconnection can happen inside the flux rope and thus accelerate electrons inside the rope.^[85,86]

Magnetic flux ropes would interact with each other during reconnection. One flux rope inevitably compresses with another flux rope inside the diffusion region, which leads to an

induced current layer between them. Then, the reconnection could happen inside this induced current layer. Sometimes, it is called re-reconnection in the magnetotail. This kind of flux rope interaction denotes the coalescence. The flux rope coalescence has been verified inside the diffusion region.^[87] The repeated generation of flux ropes and their coalescence could dominate the reconnection evolution as proposed in recent particle in cell simulation results,^[88,89] leading to the turbulence in the X-line region. Therefore, the plasma can be energized efficiently in the turbulent reconnection. Figure 3 displays one reconnection event in the magnetotail. As the Cluster spacecraft passed through the plasma sheet (Fig. 3(d)), an ion bulk flows in the L direction reversed from tailward to earthward (Fig. 3(a)). It means that the spacecraft crossed one reconnection site from tailward to earthward. B_M was closely related to B_L (Figs. 3(c) and 3(d)). They are anti-correlated in the tailward flows and positively correlated in the earthward flows, consistent with the expected Hall magnetic field inside the ion diffusion region. In the diffusion region of this event, a large number of bipolar signatures of B_N were detected and accompanied with enhancement of B_M at the same time. It indicates that there existed many magnetic flux ropes inside the diffusion region. By investigating all the interaction region between any two adjacent flux ropes, we identified a few coalescence events, because the reconnection was ongoing in the induced electric field of the interaction region. Thus, the reconnection diffusion region evolved into turbulence.

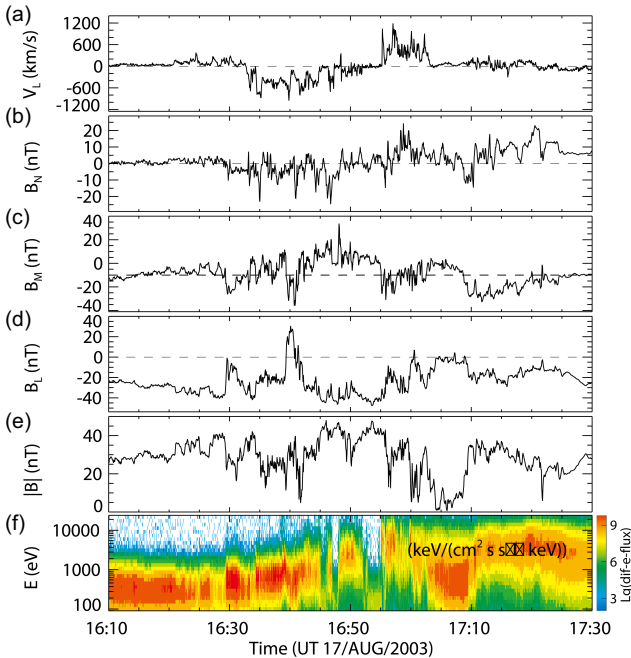


Fig. 3. A reconnection event in the magnetotail in the local current coordinate system:^[87] (a) ion bulk flow in the L direction, (b)–(e) three components and magnitude of magnetic field, (f) ion energy–time spectrum.

Mostly recently, Magnetospheric Multiple (MMS) mission launched by NASA can provide the unprecedented high time resolution measurement for the plasma and thus make

the detection of the electron diffusion region available.^[36] The observations shows that the electron diffusion region has a few striking features in the magnetotail.^[90–95] First of all, the electron frozen-in condition is broken inside the electron diffusion region and the deviation between the measured electric field (\mathbf{E}) and the electron convection term ($\mathbf{V}_e \times \mathbf{B}$) is mainly caused by the divergence of electron pressure tensor. Secondly, the electrons display the agyrotropy and crescent distribution in the plane perpendicular to magnetic field lines but isotropic distribution in the neutral sheet. Thirdly, the positive energy dissipation from magnetic field to plasma ($\mathbf{J} \cdot (\mathbf{E} + \mathbf{V}_e \times \mathbf{B}) > 0$). Recent observations found that the electron flows are laminar although the electric fluctuations are observed, and no energetic electrons inside the electron diffusion region.^[91]

One surprising finding is the electron diffusion region without ion-coupling in the magnetotail.^[96] By comparing with the classical electron diffusion region with ion-coupling, we found that the electron diffusion region without ion coupling could be initial stage of the reconnection, dubbed as the electron phase or “electron-only” reconnection. As the electrons are continuously energized and the electron current layer broadens, the ions would be coupled gradually.^[97,98] Namely, this kind of “electron-only” reconnection will eventually evolves into the ion phase, corresponding to the bursty reconnection.^[99] The evolution has been successfully simulated by the global PIC simulations.^[100]

2.2. Structures and physical processes in the downstream

Magnetic reconnection in the magnetotail can produce transient flow structures (such as bursty bulk flow and vortex), transient magnetic structures (such as dipolarization front, flux rope, and magnetic hole), and transient electrostatic structures (such as electron hole and electric double layer) in the downstream region. These structures play crucial roles in the flux transport, energy conversion, particle acceleration, and turbulence development in space environment. Thus, they are ideal laboratories for exploring the plasma physics and monitoring the space environment, as specified below.

The bursty bulk flow (BBF), sometimes referred to as reconnection jet^[101] or flow burst,^[44,102] is a direct consequence of the magnetotail reconnection. Such flow structure is three-dimensional^[103,104] and Alfvénic;^[101] it has typical scale of 2–3 R_E ,^[105,106] propagates both earthward and tailward,^[107,108] carries large amounts of energies from the Earth’s magnetotail to the inner magnetosphere,^[109] produces a substorm current wedge,^[110–112] and finally stops near the geosynchronous orbit.^[113,114] Usually, the frozen-in/magnetization condition is satisfied inside the BBF,^[115] but in the presence of super-Alfvénic electron jet such frozen-in condition can be broken.^[116] Considering that the magnetotail reconnection is firstly triggered in the high-density plasma

sheet region but then develops mainly in the low-density lobe region,^[117,118] the resultant BBF usually has higher temperature and lower density than the ambient plasmas.^[44,119] Such a low-entropy BBF is not conductive, and thus it interrupts the cross-tail current to form a current wedge.^[120,121] Therefore, the BBF plays a key role in the initiation of magnetospheric substorm^[46] and the lightning of ionospheric aurora.^[47,122] Moreover, it plays a key role in the initiation of magnetic storm,^[123] because the thermal ions carried by such BBF can inject to the inner magnetosphere to significantly enhance the ring current,^[124,125] and plays a key role in the formation of radiation belts,^[126,127] because the thermal electrons carried by the BBF can act as a “seed” of relativistic electrons when they are injected to the inner magnetosphere.^[128] Inside the BBF, energetic electrons,^[129] energetic ions,^[130] kinetic Alfvén waves,^[131] lower hybrid waves,^[116,132] slow magnetosonic waves,^[133] and compressible turbulence^[134] have been widely reported.

The vortex, characterized by a ring-like flow pattern, is also a consequence of magnetotail reconnection.^[135] Such structure can have scale from the ion inertial length^[136,137] to the MHD scale;^[138] it prefers to appear at the edge of reconnection jets or BBFs,^[139] and thus it is quite possibly generated by the interchange instability^[140] or flow braking/rebound^[141] during the propagation of BBFs. The large-scale vortex near the flow-braking region (around $X_{\text{GSM}} = -8R_E$) may contribute to the formation of the region-I field-aligned current,^[142] and thus it is an important ingredient of the magnetospheric substorm. A recent study^[143] shows that the flow vortex actually is an isobaric structure and can cause significant electron heating and electrostatic turbulence inside it. Compared to other transient structures produced by magnetic reconnection, the vortex has not been well studied hitherto, due to the lack of efficient analysis tools. Fortunately, recently the First-Order Taylor Expansion of Velocity (FOTEV) method has been developed.^[144] Such method is very powerful and will greatly improve our understanding of the vortex properties in the future.

The dipolarization front (DF) is a transient magnetic structure produced by the magnetotail reconnection,^[145,146] so it is also termed “reconnection front”.^[147] Such structure is characterized by a sudden increase of magnetic field B_z in GSM coordinates,^[148–150] preceded by a small B_z dip structure,^[151–153] and followed by a strong B_z region that is termed flux pileup region (FPR)^[154–156] or dipolarizing flux bundle (DFB);^[157,158] it has a typical azimuthal scale of 2–3.6 R_E in the equatorial plane^[148] and a vertical scale of 1.5–2 R_E in the meridian plane^[105] — on the order of MHD scale, and has a typical thickness of 500 km–1000 km^[159,160] — on the order of ion inertial length,^[161,162] but can include fine structures^[147,163] — on the order of electron inertial

length;^[164–167] it can appear extensively in the whole magnetotail from $X_{\text{GSM}} \approx -30R_E$ to $X_{\text{GSM}} \approx -6R_E$ ^[157,161,162,168] with a saddle-like configuration,^[115,157,169] but preferably appears in the magnetotail transition region at $X_{\text{GSM}} \approx -15R_E$,^[162] where the stretched tail-like magnetic field line transforms to a more dipole-like shape and the plasma flow starts to brake;^[170] it can propagate both earthward and tailward,^[145,171] with the earthward DF typically much steeper than the tailward DF.^[172] Inherently, the DF is a tangential discontinuity^[113,173] separating hot tenuous plasmas (convection from the reconnection site) from cold dense plasmas in the Earth’s magnetotail. Immediately ahead of the DF, plasmas are also hot. However, these hot plasmas are actually the “precursor flows” accelerated locally at the front boundary,^[174] rather than convected from the reconnection site.

In principle, the DF can (i) transport mass and magnetic fluxes from middle magnetotail to the inner magnetosphere,^[47,158,175] (ii) generate field-aligned current in the meridian plane^[162,176,177] and interrupts the cross-tail current in the equatorial plane,^[178,179] (iii) link magnetotail dynamics with the ionospheric phenomenon,^[180–183] (iv) converts magnetic energy to particle energy^[147,164,165,184] or inversely converts particle energy to magnetic energy,^[185] (v) excite various plasma waves.^[124,186–195]

Apart from these roles, the most important role of DFs probably is the electron acceleration.^[118,155,196–210] Such acceleration can be categorized into global and local processes (in terms of the place where the acceleration happens) or categorized into adiabatic and nonadiabatic processes (in terms of the conservation/violation of magnetic moment). Typically, the global-scale process, including Fermi and betatron acceleration,^[165,209,211,212] is adiabatic, whereas the local process can be either adiabatic (betatron acceleration^[155,196]) or nonadiabatic (wave-particle interaction^[190,191]). These four types of electron acceleration (global-scale Fermi acceleration, global-scale betatron acceleration, local betatron acceleration, local wave-particle interaction) are attributed to different mechanisms: Specifically, (I) the global-scale Fermi acceleration is caused by the shrinking of magnetic field lines between the two mirror points of electron bounce, which happens during the earthward propagation of DFs from middle magnetotail to the inner magnetosphere;^[155] (II) the global-scale betatron acceleration is caused by the spatial enhancement of magnetic fields, which happens during the earthward propagation of DFs from middle magnetotail (weak- B region) to the inner magnetosphere (strong- B region);^[212] (III) the local betatron acceleration is caused by the temporal enhancement of magnetic fields, which happens when the magnetic flux tubes behind the DF are contracting;^[155,196] (IV) the local wave-particle interaction is caused by the cyclotron resonance, which happens when the whistler waves

are present and simultaneously the cyclotron-resonance condition between electrons and waves is satisfied.^[213,214] In principle, these four types of acceleration can work individually or together. Inside a decaying FPR, where the flow velocity is decreasing and flux tubes are expanding, the global-scale Fermi acceleration is dominant (see the left column of Fig. 4), whereas inside a growing FPR, where the flow velocity is increasing and flux tubes are contracting, the local betatron acceleration is dominant (see the right column of Fig. 4). If the Fermi acceleration is dominant behind DFs, it will result in the “cigar-type” pitch-angle distribution (showing electron pitch angles primarily at 0° and 180°). On the contrary, if the betatron acceleration is dominant, it will result in the “pancake-type” pitch-angle distribution (showing electron pitch angles primarily at 90°). Interestingly, if the Fermi acceleration and betatron acceleration are both prominent behind DFs, a new type of electron pitch-angle distribution (termed the “rolling-pin” distribution, showing electron pitch angles primarily at 0° , 90° , and 180°) will be formed.^[215,216] Such

rolling-pin distribution has been widely observed by spacecraft behind DFs^[197,198,200,215–219] and well re-produced in simulations.^[220–223] Interestingly, this kind of rolling-pin distribution is very sensitive to the shape of the FPR (or actually the magnetic bottle behind the DF):^[198] when the FPR is a “fat bottle”, the rolling-pin distribution is very clear; when the FPR is a “slim bottle”, the rolling-pin distribution disappears (see the spacecraft observations and schematic illustration in Fig. 5). Commonly, behind the DF, the global-scale electron acceleration is more prominent than the local electron acceleration,^[212] whereas in certain circumstances the local electron acceleration can be more prominent than the local electron acceleration.^[197] Taking into account both the global-scale and local accelerations, the earthward-propagating DF can lead to an enhancement of energetic-electron fluxes up to 10000 times during 30 seconds,^[118] which is even more efficient than the electron acceleration in the radiation belts.^[224] This is probably the reason why relativistic electrons can be directly observed during the magnetotail dipolarization.^[225]

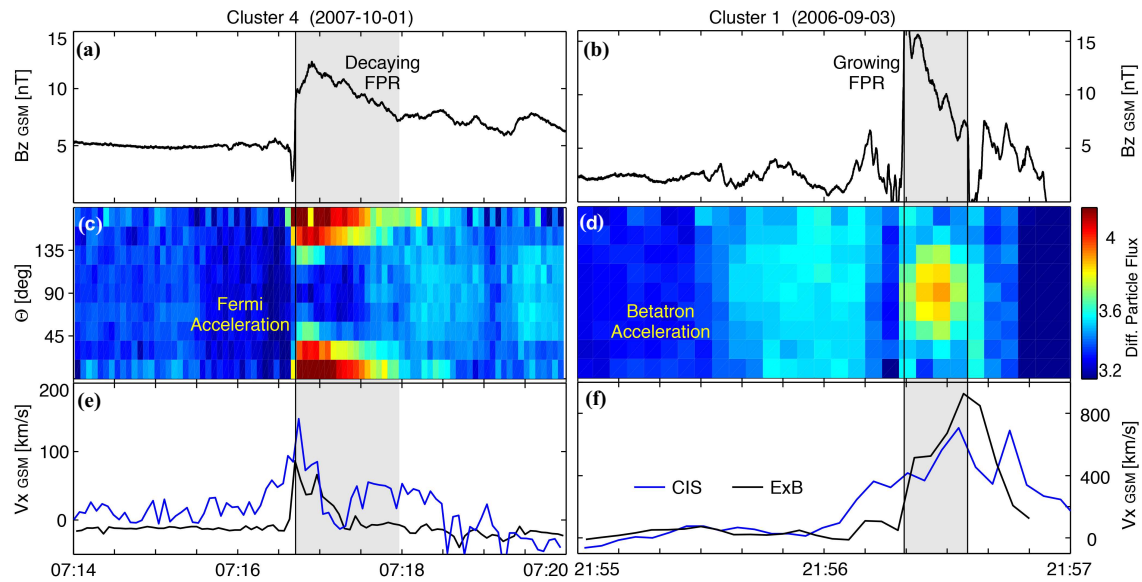


Fig. 4. A comparison of the Fermi and betatron acceleration behind dipolarization fronts (DFs). Specifically, Fermi acceleration happened on 2007-10-01, when the flow velocity was decreasing behind DFs; betatron acceleration happened on 2006-09-03, when the flow velocity was increasing behind DFs. (Modified from Fu *et al.*^[155]).

The magnetic hole (MH) is another transient product of the magnetotail reconnection. Such structure is characterized by a significant drop of magnetic strength without the change of magnetic-field direction.^[226,227] To some degree, this signature is similar to the partial crossing of the neutral sheet by a spacecraft, so that in spacecraft measurements the identification of the MH should be very careful. Typically, the MH structure can have scale from electron inertial length^[136] to ion inertial length.^[228] The different scale of MHs indicates different plasma properties: Inside a large-scale MH, the electron density increases, whereas the electron temperature may not change;^[228] inside an electron-scale MH, the electron density may not change, whereas the electron perpendicular tempera-

ture significantly increases.^[229,230] Quite frequently, the MH is observed inside the strong-Bz region in the reconnection jet.^[231] Its formation mechanism may be related to mirror-mode instabilities^[231] or interchange instabilities.^[229] Important roles of MHs in the magnetotail are the trapping of energetic electrons^[230] and the excitation of whistler waves,^[232] either at the edge^[233] or in the center.^[234,235] To uncover the inheritance of MHs comprehensively, the Second-Order Taylor Expansion (SOTE) method is a useful tool.^[236,237]

In the downstream region of the magnetotail reconnection, electrostatic transient structures can also be formed, in addition to the magnetic and flow structures. In particular, electron holes (EHs) and double layers (DLs) are two elec-

trostatic transient structures frequently observed in the reconnection jet. These two structures both have the Debye scale, with the EH characterized by a bipolar variation of parallel electric fields^[238–241] and the DL characterized by a unipolar variation of parallel electric fields.^[242,243] In this sense, sometimes the EH is termed electrostatic solitary wave (ESW). Typically, these two electrostatic structures propagate rapidly, with a speed larger than the local Alfvén velocity.^[244–246] The interior dynamics of such structures has been a mystery, unless the recent observation by the MMS spacecraft.^[247] In certain circumstances (*e.g.*, structure propagation in the direction opposite to BBF), the EH and DL can have very slow speed in the spacecraft frame,^[154,247] and thus the high-resolution measurements of the interior of these structures are possible. For many years, scientists expect significant electron acceleration inside EHs.^[248] However, the recent observation found that there is no electron and ion acceleration inside the EH,^[247] which may challenge the conventional theory.

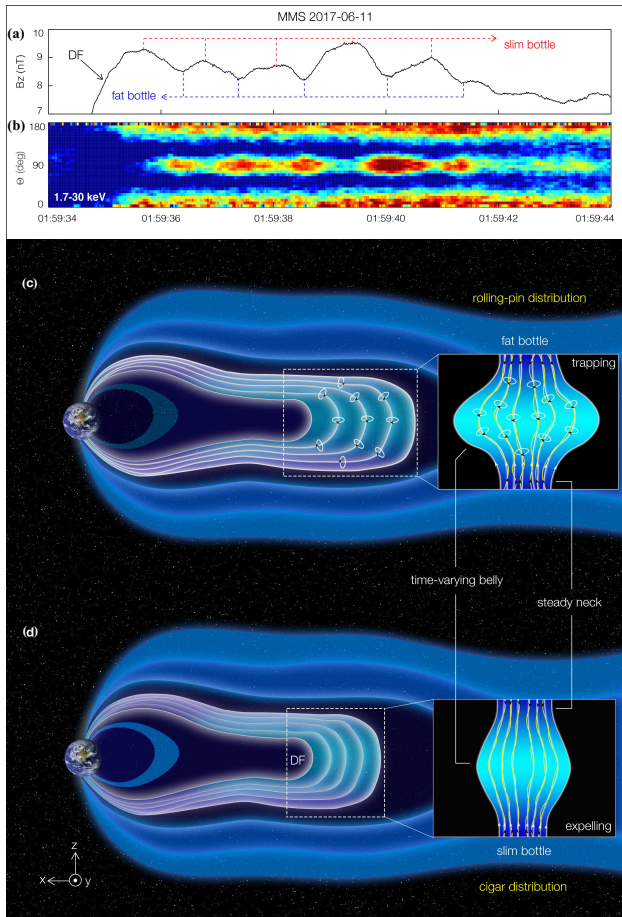


Fig. 5. Spacecraft observations and schematic illustration of the evolution of electron rolling-pin distribution behind DFs. Specifically, if the magnetic bottle behind the DF is “fat” (indicated by the weak magnetic fields in spacecraft measurements), a rolling-pin distribution is formed; if the magnetic bottle behind the DF is “slim” (indicated by the strong magnetic fields in spacecraft measurements), the rolling-pin distribution disappears. (Modified from Fu *et al.*^[198]).

As products of magnetic reconnection in the downstream region, these transient structures (including magnetic, electro-

static, and flow) are very dynamic. They act as a medium for the magnetic reconnection to impact space environment, and thus they are crucial factors during the space-weather forecast. To better understand the inheritance of these structures, recently a few spacecraft missions (*e.g.*, AME^[249] and Plasma Observatory^[250]) have been proposed. The launch of these missions will greatly improve our understating of the downstream structures and processes of magnetic reconnection in space.

3. Magnetic reconnection in the magnetopause

The magnetopause is a sharp boundary between the shocked solar wind in the magnetosheath and the magnetosphere. The shocked interplanetary magnetic field in the magnetosheath can reconnect with the geomagnetic field at the magnetopause. Without magnetopause reconnection, the Earth’s magnetosphere is a relatively isolated space from the solar wind. Magnetopause reconnection opens up the magnetopause, allowing penetration of solar wind plasmas and energy into the magnetosphere, therefore, it is the origin of the energy conversion processes in Earth’s magnetosphere. It should be noted that the plasma density and temperature and the magnetic field are different on the magnetosheath and magnetosphere sides of magnetopause reconnection, and thus the magnetopause reconnection is asymmetric. In the follows, we will at first focus on the diffusion region and particle kinetics of magnetopause reconnection, and then zoom out to discuss the manifestations and consequences of reconnection at low- and high-latitude magnetopause, respectively.

3.1. Diffusion region and particle kinetics

From 2000s, *in-situ* spacecraft began to observe magnetopause reconnection. Deng and Matsumoto^[25] reported Geotail observations of magnetopause reconnection, showing the features of the Hall current and the Hall magnetic field in the ion diffusion region. Mozer *et al.*^[251] reported Polar satellite observations of the Hall signatures in the ion diffusion region of magnetopause reconnection, and then Mozer *et al.*^[252] further reported Polar observations of the electron diffusion region of magnetopause reconnection. The above diffusion regions of magnetopause reconnection were observed by single-spacecraft (Geotail, Polar), the Cluster mission allowed for the first time four-spacecraft observations of the diffusion regions, so that spatial and temporal features can be distinguished reliably. Vaivads *et al.*^[253] reported Cluster observations of a diffusion region of magnetopause reconnection, and they measured a fast reconnection rate of ~ 0.1 and showed the dominance of Hall physics in the ion diffusion region, which are in agreement with the standard collisionless reconnection model.^[2,4,15,16]

The above early *in-situ* detections of magnetopause reconnection mostly paid attention to the basic structures, whereas the asymmetry was overlooked. Therefore, the standard model of collisionless reconnection needs to be modified by taking into account the asymmetries between the magnetosheath and magnetospheric sides to better describe magnetopause reconnection.^[66,254–260] Cassak and Shay^[256] theoretically derived scaling laws for the reconnection rate, outflow speed, the density of the outflow, and the structure of the diffusion region. They also pointed out that for asymmetric reconnection, the stagnation point and the X-line are not colocated, and then they verified the scaling laws with 2D MHD simulations. Using 2D PIC simulations, Pritchett^[257] found that the reconnection rate of asymmetric reconnection is smaller by a factor of 2–3 than that of symmetric reconnection, but when an external driving electric field is added, the reconnection rate increases substantially. They further demonstrated the characteristics of electron and ion flows and electromagnetic fields that are asymmetric between the magnetosheath and magnetospheric sides, as shown in Fig. 6. Motivated by the above theoretical and simulation studies, observers began to pay attention to the asymmetric structures in magnetopause reconnection.^[261–264]

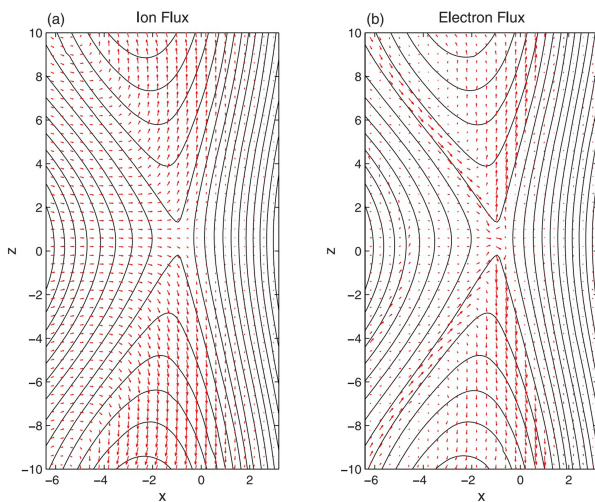


Fig. 6. Ion and electron fluxes (nV represented by arrows) obtained from a particle-in-cell simulation of magnetopause reconnection.^[257] The solid lines represent projections of the magnetic field lines onto the reconnection plane.

The high-resolution, four-spacecraft observations by MMS significantly expedite the understanding magnetopause reconnection, especially its electron diffusion region. At the same time, simulations have also been improved to echo the MMS observations.^[265–273] Burch *et al.*^[274] reported the first MMS observations of an electron-diffusion region of magnetopause reconnection, which showed the conversion of magnetic energy to particle energy caused by the electric field and current therein. They also showed the crescent-shaped electron velocity distribution and identified the electron population resulted from demagnetization and acceleration by

reconnection. MMS observations have also shown particle acceleration and fine structures of current and electromagnetic field in the reconnection exhaust and the ion diffusion region.^[275–287] In addition, various types of plasma waves and turbulences have been observed by MMS at magnetopause reconnection,^[132,244,288–293] but the role of them in reconnection remains unclear, which needs further studies.

3.2. Low-latitude magnetopause reconnection

When the interplanetary magnetic field has a southward component, it can reconnect with the northward geomagnetic field at the low-latitude magnetopause, as predicted by Dungey.^[294] Such low-latitude magnetopause reconnection began to draw more attention because it had been believed to cause the flux transfer events (FTEs) discovered by Russell and Elphic.^[295] Initially, FTEs were thought to be flux tubes that are produced by single X-line reconnection between the IMF and the geomagnetic field.^[295] However, Lee and Fu^[296] suggested that FTEs are essentially magnetic flux ropes formed by multiple X-line reconnection. In addition to these two models, other alternative models were also proposed to interpret the formation of FTEs. For example, Scholer^[297] suggested that FTEs are essentially loop-like field lines formed by non-stationary single X-line reconnection.

These models had been controversial until the *in-situ* observations by the Cluster and THEMIS spacecraft provided evidence for the multiple X-line reconnection model. By applying the Grad–Shafranov reconstruction technique to the FTEs observed by Cluster, Hasegawa *et al.*^[298] showed that the reconstructed FTEs consisted of one or more magnetic flux ropes, suggesting that multiple X-line reconnection was involved in the formation of the FTEs. Later, using THEMIS observations, Hasegawa *et al.*^[299] provided direct evidence for an FTE formed by multiple X-line reconnection at the low-latitude magnetopause. The evidence consists of i) two oppositely-directed ion jets converging towards the FTE, ii) the cross-section of the FTE core being elongated along the magnetopause normal, probably squeezed by the oppositely-directed jets, and iii) bidirectional field-aligned fluxes of energetic electrons in the magnetosheath, indicating reconnection on both sides of the FTE. Øieroset *et al.*^[300] and Zhong *et al.*^[301] also reported detections of magnetic flux ropes flanked by multiple magnetic reconnection X-lines at the low-latitude magnetopause, which further supported the multiple X-line reconnection model of FTEs. Given the above evidence, it has now been widely accepted that FTEs are essentially magnetic flux ropes formed by multiple X-line reconnection at the low-latitude magnetopause.

Global-scale simulations have been performed to better understand structure and evolution of the low-latitude magnetopause reconnection and flux ropes as FTEs. Early global

simulations were mostly magnetohydrodynamic (MHD). Raeder^[302] reported the formation of FTEs (flux ropes) between multiple X-lines in a global MHD simulation with a large dipole tilt angle, and they found no FTE formed when the dipole tilt angle is zero. However, the global MHD simulations by Dorelli and Bhattacharjee^[303] and Glocer *et al.*^[304] showed that FTEs can still form without a dipole tilt. Sun *et al.*^[305] and Chen *et al.*^[306] presented large-scale characteristics of FTEs in the dayside magnetopause by using global MHD simulations. Using the more advanced multifluid global MHD simulations, and Winglee *et al.*^[307] also showed the formation of FTEs by multiple X-line reconnection. Note that MHD simulations do not include particle kinetics, and thus cannot resolve the fast magnetopause reconnection and kinetic-scale FTEs. One way to include particle kinetics into global-scale simulations is to embed a domain of particle-in-cell (PIC) simulation into a global MHD simulations because PIC simulations treat ions and electrons as full particles.^[281,282]

The other way is to use hybrid simulations which resolve ion kinetics and ignore electron kinetics. The global hy-

brid simulations were firstly performed with 2D codes.^[308–311] The first 3D global hybrid simulation of the low-latitude magnetopause reconnection and FTEs was performed by Tan *et al.*,^[312] in which they showed a quadrupolar magnetic field signature associated with the Hall effect (*i.e.*, decoupling between the motions of ions and electrons) around the FTEs. They also showed that the X-lines have a finite length, and the ions trapped by the FTEs so that the density is enhanced in the FTEs. Tan *et al.*^[313] further studied ion precipitation associated with magnetopause reconnection and FTEs. Using 3D global hybrid simulations, Guo *et al.*^[314,315] further showed that the magnetopause flux ropes (*i.e.*, FTEs) can coalesce with each other and with the cusp magnetic field through 3D re-reconnection processes, and they also show that these processes depend on the orientation of the IMF. The 3D re-reconnection process is during flux rope coalescence is shown in Fig. 7. These 3D re-reconnection processes lead to an increase in the magnetic flux connected to the Earth, which favors particle and energy transport to the magnetosphere.

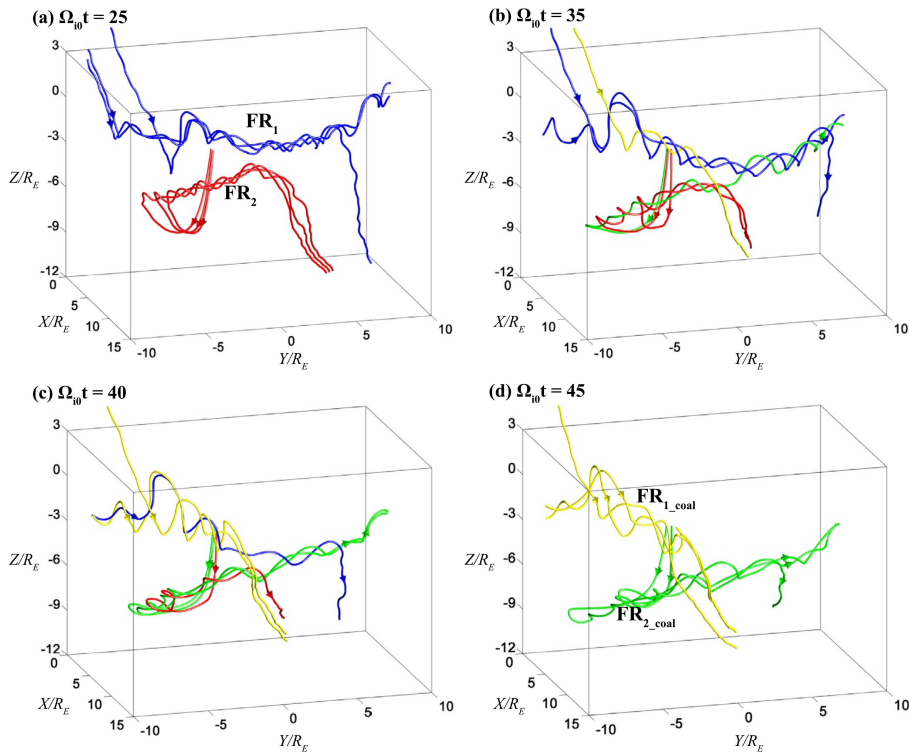


Fig. 7. Three-dimensional re-reconnection process during coalescences between two magnetopause flux ropes in a global hybrid simulation.^[314] The curves are representative magnetic field lines, and the different colors represent different field line topologies.

3.3. High-latitude magnetopause reconnection

When the IMF is northward, magnetopause reconnection can still occur, not at low-latitude but at high latitude, between the IMF and the open field lines of the tail lobe, as predicted by Dungey.^[316] The first *in-situ* detection of such reconnection was reported by Gosling *et al.*^[317] using ISEE 2 observations. Such reconnection between the IMF and the open field

lines of the tail lobe can occur in both northern and southern hemispheres, which forms new closed field lines at the dayside magnetopause that are favorable for the formation of the low-latitude boundary layer under northward IMF.^[318] It has been well accepted that the magnetosphere is much quieter under northward IMF than southward IMF. However, Shi *et al.*^[319] reported that high-latitude magnetopause reconnection may still be able to allow solar wind entry into the magnetosphere

during geomagnetic quiet times. Moreover, such high-latitude magnetopause reconnection can cause particle precipitation from the solar wind into the magnetosphere, leading to day-side aurora, as shown by the simultaneous observations of reconnection and proton auroral spot.^[320,321] In addition to the high-latitude reconnection between the northward IMF and the open field lines of the tail lobe (usually tailward of the cusp), there is another high-latitude magnetopause reconnection between the northward IMF and the closed geomagnetic field lines occurring earthward of the cusp.^[322–324]

A key question for the high-latitude magnetopause reconnection was that whether it can occur at multiple X-lines and form magnetic flux ropes as in low-latitude magnetopause reconnection. Satellite observations indicated that under the northward IMF, the high-latitude magnetopause reconnection occurs at a single X-line and no flux ropes are formed.^[325] However, Zong *et al.*^[326] reported Cluster observations of a plasmoid-like structure in the high-latitude magnetopause under the northward IMF. The plasmoid is similar to the flux rope (except for the absence of the core field), and it suggests that the high-latitude magnetopause reconnection can occur at multiple X-lines. Also using Cluster observations, Hasegawa *et al.*^[327] showed that magnetopause reconnection can retreat tailward, which was accompanied by formation of a new X-line, leading to multiple X-line reconnection.

Global-scale simulations help better understand the high-latitude magnetopause reconnection under northward IMF. Using 3D global MHD simulations, Berchem *et al.*^[328] showed the formation of magnetic flux ropes, suggesting the occurrence of multiple X-line reconnection. Using 2D global hybrid simulations, Grandin *et al.*^[329] further studied the plasma signatures of the high-latitude magnetopause flux ropes formed by multiple X-line reconnection. More recently, Guo *et al.*^[330] performed 3D global hybrid simulations to study high-latitude magnetopause reconnection and flux ropes under northward IMF. They found that the aforementioned two types of high-latitude magnetopause reconnection (both tailward and earthward of the cusp) can occur almost simultaneously. The 3D global hybrid simulations also showed that high-latitude magnetopause flux ropes with four different topologies of magnetic field lines can be formed by multiple X-line reconnection. The core field and the location of the flux ropes was found to depend on the IMF B_y component – when the IMF B_y is zero, the flux ropes have a weak core field (*i.e.*, resembles plasmoids) and are located at the noon-midnight meridian plane; when the IMF B_y is positive (negative), the flux ropes begin to have a nonzero core field, and they shift duskward (dawnward) in the northern hemisphere (oppositely in the southern hemisphere).

4. Magnetic reconnection in the magnetosheath

A bow shock is formed in front of the Earth's magnetosphere after its interaction with the high-speed, super-Alfvénic solar wind. The bow shock consists of two parts: a quasi-perpendicular shock where the shock angle θ_{Bn} between the shock normal and upstream magnetic field is larger than 45° , and a quasi-parallel shock where the shock angle θ_{Bn} is smaller than 45° . The magnetosheath downstream of a quasi-perpendicular shock is quite different from that of a quasi-parallel shock.^[331–339]

In a quasi-parallel shock, the reflected ions by the shock can move along the magnetic field to reach the far upstream, and the magnetosonic waves are then excited by the plasma beam instability. Although the excited waves have a propagation velocity toward the upstream in the plasma frame, they are convected toward the shock by the solar wind. These large amplitude magnetosonic waves are highly compressed after they penetrate through the shock and enter the magnetosheath, which is in a turbulent state.^[340–343] Current sheets are then formed in the magnetosheath, and magnetic reconnection may consequently occur in these turbulent current sheets.^[32,33,344–349] The first *in-situ* observational evidence of magnetic reconnection in the magnetosheath downstream of the quasi-parallel shock with Cluster spacecraft was provided by Retino *et al.*,^[32] and the width of the current sheet is about one ion inertial length. In this reconnection event, a quadrupolar structure of the out-of-plane magnetic field is identified, and the reconnection rate is estimated to be 0.1. All these evidences have demonstrated that this is a typical collisionless magnetic reconnection event, which has been ubiquitously observed in the magnetotail. From then on, more ion-scale reconnection events have been observed by in the Earth's magnetosheath with both Cluster and MMS spacecraft, and electrons may be heated and accelerated.^[33,344,349] By performing 3D global hybrid simulations, Lu *et al.*^[347] proposed that the current sheets in the magnetosheath behind the parallel shock is formed after the upstream large-amplitude electromagnetic waves penetrate through the shock and are then compressed in the downstream. Recently, Phan *et al.*^[345] reported an electron-scale reconnection event in the magnetosheath downstream of a quasi-parallel shock as shown in Fig. 8. Different from the standard collisionless reconnection, where an electron-scale thin current sheet with about several electron inertial lengths is embedded in an ion-scale current sheet, there is only an electron-scale current sheet. In the electron-scale reconnection event, there exists bi-directional super-ion-Alfvénic electron jets and parallel electric field, but obvious ion jets. This kind of reconnection is also called as “electron-only” reconnection. The findings reveal that magnetic reconnection works different when the current sheet is sufficiently small.^[349] Please note that “electron-only” reconnection in

the magnetosheath is different from that in the magnetotail. “Electron-only” in the magnetotail is a transient phase,^[96,100] which at last will evolve to an ion phase, while “electron-only” reconnection in the magnetosheath can persist for a long time.

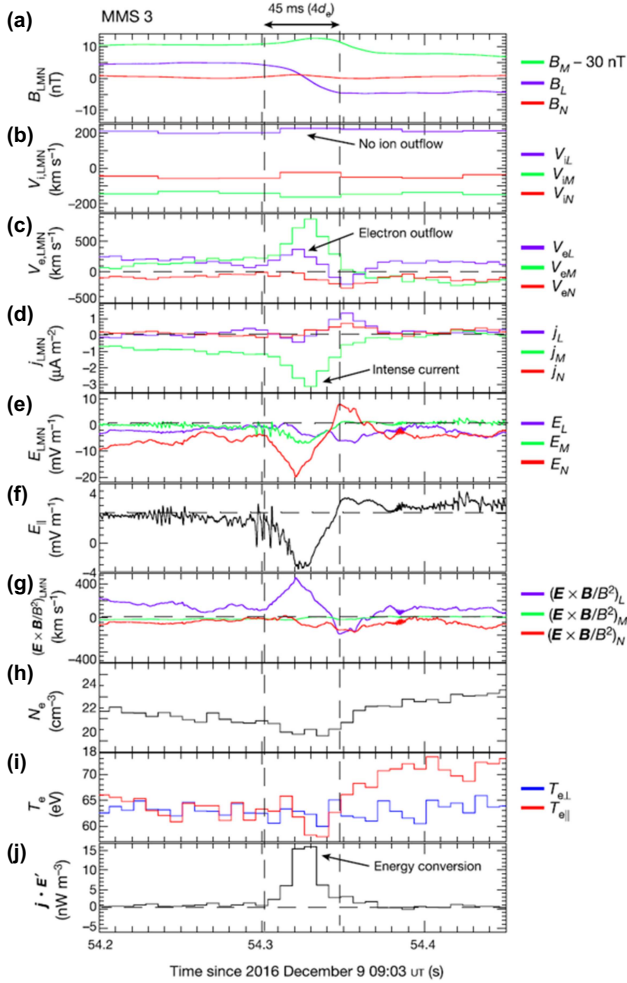


Fig. 8. MMS 3 observation of an electron-scale current sheet, and the data are shown in a common current-sheet (LMN) coordinate system, determined for the MMS 3 crossing of the current sheet at 09:03:54.270–09:03:54.365 UT.^[345] The vertical dashed lines mark the left and right edges of the current sheet. (a) Magnetic field B_{LMN} with B_M shifted by -30 nT, (b) ion bulk velocity V_{iLMN} , (c) electron bulk velocity V_{eLMN} , (d) current density j_{LMN} from plasma measurement, (e) electric field E_{LMN} , (f) electric field E_{\perp} , (g) $(\mathbf{E} \times \mathbf{B}/B^2)$ velocity, (h) electron density N_e , (i) electron temperature T_e , (j) $\mathbf{j} \cdot \mathbf{E}' + \mathbf{V}_e \times \mathbf{B} = \mathbf{j} \cdot \mathbf{E}'$.

Although there is no large-amplitude low frequency electromagnetic waves associated with a quasi-perpendicular shock, Wang *et al.*^[350] also observed an ion-scale reconnection event in the transition region, which exhibits the typical Hall current and field pattern. By performing a 2D PIC simulation of quasi-perpendicular shock, Lu *et al.*^[351] found that when the reflected ions by the shock turn around and then move toward the shock, the magnetic field lines begin to bend around the shock and then form current sheets, and at last magnetic reconnection occurs.

The current sheets in the magnetosheath are associated with the large-amplitude magnetic fluctuations, and their widths can range from ion inertial length to electron inertial

length. Both ion-scale reconnection and electron-scale reconnection can be observed in the magnetosheath, which exhibits the different characteristics from those in the magnetotail and magnetopause, and their roles in the transfer of momentum and energy from the solar wind to the magnetosphere need further investigation.

5. Summary

In this paper, we have reviewed the recent findings on collisionless magnetic reconnection in the earth’s magnetotail, magnetopause and magnetosheath, which are based on satellite observations including Cluster and MMS, *etc.* These findings can be described as follows:

(I) Satellite observations have demonstrated validity of the standard model of reconnection occurred in the magnetotail, magnetopause and magnetosheath, where an electron diffusion region is embedded in an ion diffusion region.

(II) The symmetry of electrons flows in the separatrix region will be deviated when there exists a guide field or reconnection is asymmetric, which leads to the structure of the out-of-plane magnetic field different from that depicted in Fig. 1.

(III) There exist various kinds of plasma waves in both the electron diffusion region and ion diffusion region, and these waves can efficiently scatter electrons although their quantitative contributions to energy dissipation in magnetic reconnection is difficult to evaluate.

(IV) Flux ropes, which may coalesce each other, are ubiquitously observed during magnetic reconnection, and can accelerate electrons.

(V) Various transient structures are produced in the downstream of magnetotail reconnection, which also contribute to energy dissipation in reconnection.

(VI) Electron-only reconnection may occur in the magnetotail and magnetosheath. In the magnetotail, electron-only reconnection may trigger the subsequent bursty release of magnetic energy. In the magnetosheath, electron-only reconnection may be the intrinsic characteristics of turbulent reconnection.

Because of the small separation between satellites and availability of only *in-situ* observations in the missions like Cluster and MMS, our understanding on global physics of magnetic reconnection at the Earth is still very limited although great advances on kinetic physics of magnetic reconnection have been achieved. The upcoming spacecraft mission, like the Solar wind Magnetosphere Ionosphere Link Explorer (SMILE),^[352] which will be launched in 2024 and can provide the global image of the Earth’s magnetosphere, may help us understand the global physics of magnetic reconnection.

In addition to the Earth’s magnetosphere, magnetic reconnection may occur in other planets, solar atmosphere, or even

the astrophysical system, where the range of the scale size is huge. If we define a normalized parameter $D = L/d_i$ (where L is the scale size of current sheet in magnetic reconnection, and d_i is the ion inertial length. At the earth, D is about 500), then D may change from about 50 to larger than 10^8 . When D is small, like at the Mercury ($D \sim 50$), satellite observations have shown that kinetic physics is important. But when D is larger, like in the solar atmosphere ($D \sim 10^{6-7}$), whether kinetic physics still plays an important role is still a puzzle.^[4] One can anticipate that in such a large scale current sheet a hierarchy of flux ropes and new current sheets is formed, while the smallest scale size of flux ropes and current sheets can extend down to kinetic scale, leading to energy dissipation. Validating this hypothesis, which is far beyond the present technology of satellite observation, is a grand challenge for space physicists nowadays.

Acknowledgments

Project supported by the National Natural Science Foundation of China (Grant No. 42174181), the Strategic Priority Research Program of the Chinese Academy of Sciences (Grant No. XDB 41000000), and the Key Research Program of Frontier Sciences, Chinese Academy of Sciences (Grant No. QYZDJ-SSW-DQC010).

References

- [1] Biskamp D 2000 *Magnetic Reconnection in Plasmas* (Cambridge: Cambridge University Press)
- [2] Birn J and Priest E R 2007 *Reconnection of magnetic fields: Magnetohydrodynamics and collisionless theory and observations* (Cambridge: Cambridge Univ. Press)
- [3] Yamada M, Kulsrud R and Ji H T 2010 *Rev. Mod. Phys.* **82** 603
- [4] Wang S and Lu Q M 2019 *Collisionless magnetic reconnection* (Beijing: Science Press, in Chinese)
- [5] Lu Q M, Wang R S, Xie J L, Huang C, Lu S and Wang S 2011 *Chin. Sci. Bulletin* **56** 1174
- [6] Dai L, Wang C and Lavraud B 2021 *Astrophys. J.* **919** 15
- [7] Giovanelli R G 1946 *Nature* **158** 81
- [8] Tsuneta S, Hara H, Shimizu T, Acton L W, Strong K T, Hudson H S and Ogawara Y 1992 *Publ. Astron. Soc. Jpn.* **44** L63
- [9] Nishida A 1978 *Geomagnetic diagnostics of the Magnetosphere* (New York: Springer)
- [10] Angelopoulos V, McFadden J P, Larson D, et al. 2008 *Science* **321** 931
- [11] Wesson J 1997 *textitTokomaks* (New York: Oxford University Press)
- [12] Sweet P A 1958 *Electromagnetic Phenomena in Cosmical Physics* edited by B. Lehnert (London: Cambridge University Press) p. 123
- [13] Parker E N 1957 *J. Geophys. Res.* **62** 509
- [14] Birn J, Drake J F, Shay M A, et al. 2001 *J. Geophys. Res.* **106** 3715
- [15] Ma Z W and Bhattacharjee A 2001 *J. Geophys. Res.* **106** 3773
- [16] Pritchett P L 2001 *J. Geophys. Res.* **106** 3783
- [17] Lu Q M, Huang C, Xie J L, et al. 2010 *J. Geophys. Res.* **115** A11208
- [18] Kuznetsova M, Hesse M and Winske D J 2001 *Geophys. Res.* **106** 3799
- [19] Wan W G and Lapenta G 2008 *Phys. Rev. Lett.* **101** 015001
- [20] Egedal J, Ng J, Le A, Daughton W, Wetherston B, Dorelli J, Gershman D and Rager A 2019 *Phys. Rev. Lett.* **123** 225101
- [21] Lu Q M, Lu S, Huang C, Wu M Y and Wang S 2013 *Plasma Phys. Control. Fusion* **55** 085109
- [22] Huang K, Lu Q M, Wang R S and Wang S 2020 *Chin. Phys. B* **29** 075202
- [23] Fu X R, Lu Q M and Wang S 2006 *Phys. Plasmas* **13** 012309
- [24] Nagai T, Shinohara I, Fujimoto M, Hoshino M, Saito Y, Machida S and Mukai T 2001 *J. Geophys. Res.* **106** 25929
- [25] Deng X H and Matsumoto H 2001 *Nature* **410** 557
- [26] Shay M A, Drake J F, Rogers B N, et al. 2001 *J. Geophys. Res.* **106** 3759
- [27] Roger B N, Denton R E and Drake J F 2003 *J. Geophys. Res.* **108** 1111
- [28] Dai L, Wang C, Zhang Y C, Lavraud B, Burch J, Pollock C and Torbert R B 2017 *Geophys. Res. Lett.* **44** 634
- [29] Dai L 2009 *Phys. Rev. Lett.* **102** 245003
- [30] McPherron R L 1991 *Physical processes producing magnetospheric substorms and magnetic storms*, in *Geomagnetism* edited by Jacobs J (London: Academic Press) pp. 593–739
- [31] Lu S, Lu Q M, Lin Y, et al. 2015 *J. Geophys. Res.* **120** 6286
- [32] Retinò A, Sundkvist D, Vaivads A, Mozer F, André M and Owen C J 2007 *Nature Physics* **3** 235
- [33] Vörös Z, Yordanova E, Varsani A, et al. 2017 *Geophys. Res. Lett.* **122** 11442
- [34] Escoubet C P, Fehringer M and Goldstein M 2001 *Annal. Geophys.* **19** 1197
- [35] Angelopoulos V 2008 *Space Sci. Rev.* **141** 5
- [36] Burch J L, Moore T E, Torbert R B and Giles B L 2016 *Space Sci. Rev.* **199** 5
- [37] Angelopoulos V, Artemyev A, Phan T D and Miyashita Y 2020 *Nat. Phys.* **16** 317
- [38] Sergeev V, Angelopoulos V, Kubyshkina M, et al. 2011 *J. Geophys. Res.* **116** A00i26
- [39] Shen C, Liu Z X, Li X, et al. 2008 *J. Geophys. Res.* **113** A07s21
- [40] Tang C L, Li Z Y, Angelopoulos V, et al. 2009 *J. Geophys. Res.* **114** A09211
- [41] Zhou X Z, Angelopoulos V, Runov A, et al. 2009 *J. Geophys. Res.* **114** A03223
- [42] Pu Z Y, Chu X N, Cao X, et al. 2010 *J. Geophys. Res.* **115** A02212
- [43] Sonnerup B U O 1979 *Solar System Plasma Physics* edited by Lanzerotti L T, Kennel C F and Parker E N pp. 45–108
- [44] Angelopoulos V, Kennel C F, Coroniti F V, et al. 1994 *J. Geophys. Res.* **99** 21257
- [45] Cao J B, Duan J T, Du A M, et al. 2008 *J. Geophys. Res.* **113** A07s15
- [46] Ge Y S, Raeder J, Angelopoulos V, Gilson M L and Runov A 2011 *J. Geophys. Res.* **116** A00i23
- [47] Zhang M, Wang R S, Lu Q M and Wang S 2020 *Astrophys. J.* **891** 175
- [48] Oieroset M, Phan T D, Fujimoto M, Lin R P and Lepping R P 2001 *Nature* **412** 414
- [49] Ma Z W and Bhattacharjee A 1998 *Geophys. Res. Lett.* **25** 3277
- [50] Oieroset M, Lin R P, Phan T D, Larson D E and Bale S D 2002 *Phys. Rev. Lett.* **89** 195001
- [51] Wygant J R, Cattell C A, Lysak R, et al. 2005 *J. Geophys. Res.* **110** A09206
- [52] Asano Y, Mukai T, Hoshino M, et al. 2003 *J. Geophys. Res.* **108** 1189
- [53] Eastwood J P, Phan T D, Oieroset M and Shay M A 2010 *J. Geophys. Res.* **115** A08215
- [54] Chen L J, Bessho N, Lefebvre B, et al. 2008 *J. Geophys. Res.* **113** A12213
- [55] Wang R S, Lu Q M, Huang C and Wang S 2010 *J. Geophys. Res.* **115** A01209
- [56] Egedal J, Daughton W, Le A and Borg A L 2015 *Phys. Plasmas* **22** 101208
- [57] Nan J, Huang K, Lu Q M, et al. 2022 *J. Geophys. Res.* **127** e2021JA02999
- [58] Wang R S, Du A M, Nakamura R, et al. 2013 *Geophys. Res. Lett.* **40** 2511
- [59] Wang R S, Lu Q M, Du A M, et al. 2014 *J. Geophys. Res.* **119** 9952
- [60] Wang R S, Nakamura R, Lu Q M, et al. 2012 *J. Geophys. Res.* **117** A07223
- [61] Huang C, Wang R S, Lu Q M and Wang S 2010 *Chin. Sci. Bull.* **55** 718
- [62] Zhou M, Pang Y, Deng X H, Yuan Z G and Huang S Y 2011 *J. Geophys. Res.* **116** A06222
- [63] Yu X C, Lu Q M, Wang R S, et al. 2021 *J. Geophys. Res.* **126** e2021JA029609
- [64] Eastwood J P, Shay M A, Phan T D and Oieroset M 2010 *Phys. Rev. Lett.* **104** 205001
- [65] Drake J F, Shay M A and Swisdak M 2008 *Phys. Plasmas* **15** 042306
- [66] Huang C, Lu Q M, Lu S, Wang P R and Wang S 2014 *J. Geophys. Res.* **119** 798

- [67] Slavin J A, Lepping R P, Gjerloev J, *et al.* 2003 *J. Geophys. Res.* **108** 1015
- [68] Slavin J A, Lepping R P, Gjerloev J, *et al.* 2003 *Geophys. Res. Lett.* **30** 1362
- [69] Coppi B, Laval G and Pellat R 1966 *Phys. Rev. Lett.* **16** 1207
- [70] Daughton W, Scudder J and Karimabadi H 2006 *Phys. Plasmas* **13** 072101
- [71] Drake J F, Swisdak M, Schoeffler K M, Rogers B N and Kobayashi S 2006 *Geophys. Res. Lett.* **33** L13105
- [72] Lu Q M, Wang R S, Huang K and Wang S 2020 *Journal of University of Science and Technology of China* **50** 1218
- [73] Wang R S, Lu Q M, Du A M and Wang S 2010 *Phys. Rev. Lett.* **104** 175003
- [74] Eastwood J P, Phan T D, Mozer F S, *et al.* 2007 *J. Geophys. Res.* **112** A06235
- [75] Chen L J, Bhattacharjee A, Puhl-Quinn P A, *et al.* 2008 *Nat. Phys.* **4** 19
- [76] Wang R S, Lu Q M, Li X, Huang C and Wang S 2010 *J. Geophys. Res.* **115** A11201
- [77] Zhong Z H, Zhou M, Tang R X, *et al.* 2020 *Geophys. Res. Lett.* **47** e2019GL08514
- [78] Oka M, Phan T D, Krucker S, Fujimoto M and Shinohara I 2010 *Astrophys. J.* **714** 915
- [79] Wang H Y, Lu Q M, Huang C and Wang S 2016 *Astrophys. J.* **821** 84
- [80] Lu Q M, Wang H Y, Huang K, Wang R S and Wang S 2018 *Phys. Plasmas* **25** 072126
- [81] Han S X, Wang H Y and Gao X L 2022 *Chin. Phys. B* **31** 025202
- [82] Drake J F, Swisdak M, Che H and Shay M A 2006 *Nature* **443** 553
- [83] Wang R S, Lu Q M, Nakamura R, *et al.* 2016 *J. Geophys. Res.* **121** 9473
- [84] Wang S M, Wang R S, Yao S T, *et al.* 2019 *J. Geophys. Res.* **124** 1753
- [85] Wang S M, Wang R S, Lu Q M, Fu H S and Wang S 2020 *Nat. Commun.* **11** 3964
- [86] Huang C, Lu Q M, Wang R S, Guo F, Wu M Y, Lu S and Wang S 2017 *Astrophys. J.* **835** 245
- [87] Wang R S, Lu Q M, Nakamura R, *et al.* 2016 *Nat. Phys.* **12** 263
- [88] Daughton W, Roytershteyn V, Karimabadi H, *et al.* 2011 *Nat. Phys.* **7** 539
- [89] Huang C, Lu Q M, Yang Z W, Wu M Y, Dong Q L and Wang S 2011 *Nonlin. Processes Geophys.* **18** 727
- [90] Li X M, Wang R S, Lu Q M, *et al.* 2019 *Geophys. Res. Lett.* **46** 14263
- [91] Torbert R B, Burch J L, Phan T D, *et al.* 2018 *Science* **362** 1391
- [92] Zhou M, Deng X H, Zhong Z H, *et al.* 2019 *Astrophys. J.* **870** 34
- [93] Tan B B, Li W Y, Khotyaintsev Y V, *et al.* 2022 *Geophys. Res. Lett.* **49** e2021GL097573
- [94] Li W Y, Khotyaintsev Y V, Tan B B, *et al.* 2021 *Geophys. Res. Lett.* **48** e2021GL093164
- [95] Yu X C, Lu Q M, Wang R S, *et al.* 2021 *J. Geophys. Res.* **126** e2020JA028882
- [96] Wang R S, Lu Q M, Nakamura R, *et al.* 2018 *Geophys. Res. Lett.* **45** 4542
- [97] Liu D K, Lu S, Lu Q M, Ding W X and Wang S 2020 *Astrophys. J. Lett.* **890** L15
- [98] Liu D K, Huang K, Lu Q M, Lu S, Wang R S, Ding W X and Wang S 2021 *Astrophys. J.* **922** 51
- [99] Wang R S, Lu Q M, Lu S, *et al.* 2020 *Geophys. Res. Lett.* **47** e2020GL088761
- [100] Lu S, Wang R S, Lu Q M, *et al.* 2020 *Nat. Commun.* **11** 5049
- [101] Baumjohann W, Paschmann G and Lühr H 1990 *J. Geophys. Res.* **95** 3801
- [102] Angelopoulos V, Baumjohann W, Kennel C F, *et al.* 1992 *J. Geophys. Res.* **97** 4027
- [103] Nagai T, Shinohara I, Zenitani S, Nakamura R, Nakamura T K M, Fujimoto M, Saito Y and Mukai T 2013 *J. Geophys. Res.* **118** 1667
- [104] Zhou M, Ashour-Abdalla M, Deng X, Pang Y, Fu H S, Walker R, Lapenta G, Huang S Y, Xu S and Tang R 2017 *J. Geophys. Res.* **122** 9513
- [105] Nakamura R, Baumjohann W, Mouikis C, *et al.* 2004 *Geophys. Res. Lett.* **31** L09804
- [106] Cao J B, Ma Y D, Parks G, *et al.* 2006 *J. Geophys. Res.* **111** A04206
- [107] Hones E W 1979 *Space Sci. Rev.* **23** 393
- [108] Lu S, Pritchett P L, Angelopoulos V and Artemyev A V 2018 *Phys. Plasmas* **25** 012905
- [109] Cao J B, Ma Y, Parks G, Reme H, Dandouras I and Zhang T L 2013 *J. Geophys. Res.: Space Physics* **118** 313
- [110] Shiokawa K, Baumjohann W, Haerendel G, *et al.* 1998 *J. Geophys. Res.* **103** 4491
- [111] Cao J B, Yan C X, Dunlop M, *et al.* 2010 *J. Geophys. Res.* **115** A08205
- [112] Kepko L, McPherron R L, Amm O, Apatenkov S, Baumjohann W, Birn J, Lester M, Nakamura R, Pulkkinen T I and Sergeev V 2015 *Space Sci. Rev.* **190** 1
- [113] Birn J, Nakamura R, Panov E V and Hesse M 2011 *J. Geophys. Res.* **116** A01210
- [114] Yu Y, Cao J, Fu H S, Lu H and Yao Z 2017 *J. Geophys. Res.* **122** 6139
- [115] Fu H S, Khotyaintsev Y V, Vaivads A, André M and Huang S Y 2012 *Geophys. Res. Lett.* **39** L06105
- [116] Chen Z Z, Fu H S, Liu C M, Wang T Y, Ergun R E, Cozzani G, *et al.* 2019 *Geophys. Res. Lett.* **46** 5698
- [117] Vaivads A, Khotyaintsev Y V and Andre M 2011 *Ann. Geophys.* **29** 1917
- [118] Fu H S, Xu Y, Vaivads A and Khotyaintsev Y V 2019 *Astrophys. J. Lett.* **870** L22
- [119] Chen C X and Wolf R A 1993 *J. Geophys. Res.* **98** 21409
- [120] Lui A T Y, Hones E W, Yasuhara F, Akasofu S I and Bame S J 1977 *J. Geophys. Res.* **82** 1235
- [121] Lui A T Y, Mankofsky A, Chang C L, Papadopoulos K and Wu C S 1990 *Geophys. Res. Lett.* **17** 745
- [122] Henderson M G, Reeves G D and Murphree J S 1998 *Geophys. Res. Lett.* **25** 3737
- [123] Gonzalez W D, Joselyn J A, Kamide Y, Kroehl H W, Rostoker G, Tsurutani B T and Vasyliunas V M 1994 *J. Geophys. Res.* **99** 5771
- [124] Daglis I A, Thorne R M, Baumjohann W and Orsini S 1999 *Rev. Geophys.* **37** 407
- [125] Lin Y, Wang X Y, Lu S, Perez J D and Lu Q M 2014 *J. Geophys. Res.* **119** 7413
- [126] Thorne R M 2010 *Geophys. Res. Lett.* **37** L22107
- [127] Li W and Hudson M K 2019 *J. Geophys. Res.* **124** 8319
- [128] Fu H S, Cao J B, Yang B and Lu H Y 2011 *J. Geophys. Res.* **116** A10210
- [129] Duan A Y, Cao J B, Dunlop M and Wang Z Q 2014 *J. Geophys. Res.* **119** 8902
- [130] Cao J B, Duan A, Reme H and Dandouras I 2013 *J. Geophys. Res.* **118** 7226
- [131] Duan S, Dai L, Wang C, Liang J, Lui A, Chen L, He Z, Zhang Y and Angelopoulos V 2016 *J. Geophys. Res.* **121** 4316
- [132] Ren Y, Dai L, Wang C and Lavraud B 2022 *Astrophys. J.* **928** 5
- [133] Cao J B, Wei X H, Duan A Y, Fu H S, Zhang T L, Reme H and Dandouras I 2013 *J. Geophys. Res.* **118** 1659
- [134] Wang T, Cao J B, Fu H S, Meng X and Dunlop M 2016 *Geophys. Res. Lett.* **43** 1854
- [135] Hones E W, Paschmann G, Bame S J, Asbridge J R, Scopke N and Schindler K 1978 *Geophys. Res. Lett.* **5** 1059
- [136] Huang S Y, Sahraoui F, Yuan Z G, *et al.* 2017 *Astrophys. J. Lett.* **836** L27
- [137] Liu C M, Fu H S and Liu Y Y 2021 *Astrophys. J.* **911** 122
- [138] Shi Q Q, Hartinger M D, Angelopoulos V, *et al.* 2014 *J. Geophys. Res.* **119** 4274
- [139] Birn J, Hones E W, Bame S J and Russell C T 1985 *J. Geophys. Res.* **90** 7449
- [140] Pritchett P L and Coroniti F V 2010 *J. Geophys. Res.* **115** A06301
- [141] Yao Z H, Pu Z Y, Fu S Y, *et al.* 2012 *Geophys. Res. Lett.* **39** L13102
- [142] Tian A M, Shen X C, Shi Q Q, Tang B B, Nowada M, Zong Q G and Fu S Y 2016 *J. Geophys. Res.* **121** 10813
- [143] Yu Y, Fu H S, Cao J B, Liu C M and Wang Z 2022 *Astrophys. J.* **926** 22
- [144] Wang Z, Fu H S, Olshevsky V, Liu Y Y, Liu C M and Chen Z Z 2020 *Astrophys. J. Suppl. S.* **249** 10
- [145] Fu H S, Cao J B, Khotyaintsev Y V, *et al.* 2013 *Geophys. Res. Lett.* **40** 6023
- [146] Xu Y, Fu H S, Norgren C, Hwang K J and Liu C M 2018 *Phys. Plasmas* **25** 072123
- [147] Angelopoulos V, Runov A, Zhou X Z, Turner D L, Kiehas S A, Li S S and Shinohara I 2013 *Science* **341** 1478

- [148] Nakamura R, Baumjohann W, Klecker B, *et al.* 2002 *Geophys. Res. Lett.* **29** 1942
- [149] Runov A, Angelopoulos V, Sitnov M I, *et al.* 2009 *Geophys. Res. Lett.* **36** L14106
- [150] Shu Y K, Lu S, Lu Q M, Ding W X and Wang S 2021 *J. Geophys. Res.* **126** e2021JA029712
- [151] Yao Z H, Liu J, Owen C J, *et al.* 2015 *Ann. Geophys.* **33** 1301
- [152] Lu S, Artemyev A V, Angelopoulos V, Lu Q M and Liu J 2016 *J. Geophys. Res.* **121** 4269
- [153] Schmid D, Volwerk M, Plaschke F, *et al.* 2019 *J. Geophys. Res.* **124** 9963
- [154] Khotyaintsev Y V, Vaivads A, André M, Fujimoto M, Retinò A and Owen C J 2010 *Phys. Rev. Lett.* **105** 165002
- [155] Fu H S, Khotyaintsev Y V, André M and Vaivads A 2011 *Geophys. Res. Lett.* **38** L16104
- [156] Fu H S, Khotyaintsev Y V, Vaivads A, André M, Sergeev V A, Huang S Y, Kronberg E A and Daly P W 2012 *J. Geophys. Res.* **117** A12221
- [157] Liu J, Angelopoulos V, Runov A and Zhou X Z 2013 *J. Geophys. Res.* **118** 2000
- [158] Liu J, Angelopoulos V, Zhou X Z and Runov A 2014 *J. Geophys. Res.* **119** 909
- [159] Huang S Y, Fu H S, Vaivads A, Yuan Z G, Pang Y, Zhou M, *et al.* 2015 *Astrophys. Space Sci.* **357** 22
- [160] Runov A, Angelopoulos V, Zhou X Z, Zhang X J, Li S, Plaschke F and Bonnell J 2011 *J. Geophys. Res.* **116** A05216
- [161] Schmid D, Volwerk M, Nakamura R, Baumjohann W and Heyn M 2011 *Ann. Geophys.* **29** 1537
- [162] Fu H S, Khotyaintsev Y V, Vaivads A, André M and Huang S Y 2012 *Geophys. Res. Lett.* **39** L10101
- [163] Balikhin M A, Runov A, Walker S N, Gedalin M, Dandouras I, Hobará Y and Fazakerley A 2014 *J. Geophys. Res.* **119** 6367
- [164] Liu C M, Fu H S, Xu Y, Khotyaintsev Y V, *et al.* 2018 *Geophys. Res. Lett.* **45** 4628
- [165] Liu C M, Fu H S, Vaivads A, *et al.* 2018 *Geophys. Res. Lett.* **45** 556
- [166] Pan D X, Khotyaintsev Y V, Graham D B, Vaivads A, Zhou X Z, André M, *et al.* 2018 *Geophys. Res. Lett.* **45** 12116
- [167] Nakamura T K M, Umeda T, Nakamura R, Fu H S and Oka M 2019 *Phys. Rev. Lett.* **123** 235101
- [168] Liu J, Angelopoulos V, Zhang X J, Turner D L, Gabrielse C, Runov A, Li J, Funsten H O and Spence H E 2016 *J. Geophys. Res.* **121** 1362
- [169] Beyene F, Artemyev A V, Angelopoulos V and Vasko I Y 2018 *Phys. Plasmas* **25** 082901
- [170] Shiokawa K, Baumjohann W and Haerendel G 1997 *Geophys. Res. Lett.* **24** 1179
- [171] Xu Y, Fu H S, Cao J B, Liu C, Norgren C and Chen Z 2021 *Geophys. Res. Lett.* **48** e2020GL092232
- [172] Ohtani S I, Shay M A and Mukai T 2004 *J. Geophys. Res.* **109** A03210
- [173] Sergeev V, Angelopoulos V, Apatenkov S, Bonnell J, Ergun R, Nakamura R, McFadden J, Larson D and Runov A 2009 *Geophys. Res. Lett.* **36** L21105
- [174] Zhou X Z, Angelopoulos V, Sergeev V A and Runov A 2010 *J. Geophys. Res.* **115** A00103
- [175] Nakamura R, Retino A, Baumjohann W, *et al.* 2009 *Ann. Geophys.* **27** 1743
- [176] Yao Z H, *et al.* 2013 *J. Geophys. Res.* **118** 6980
- [177] Sun W J, Fu S, Parks G K, Pu Z, Zong Q G, Liu J, Yao Z, Fu H and Shi Q 2014 *J. Geophys. Res.* **119** 5272
- [178] Grigorenko E E, Sauvaud J A, Palin L, Jacquey C and Zelenyi L M 2014 *J. Geophys. Res.* **119** 6553
- [179] Grigorenko E E, Dubyagin S, Malykhin A Y, Khotyaintsev Y V, Kronberg E A, Lavraud B and Ganushkina N Y 2018 *Geophys. Res. Lett.* **45** 602
- [180] Ge Y S, Zhou X Z, Liang J, Raeder J, Gilson M L, Donovan E, Angelopoulos V and Runov A 2012 *J. Geophys. Res.* **117** A10226
- [181] Zheng H, Fu S Y, Zong Q G, Pu Z Y, Wang Y F and Parks G K 2012 *Phys. Rev. Lett.* **109** 205001
- [182] Xu Y, Fu H S, Norgren C, Toledo-Redondo S, Liu C M and Dong X C 2019 *Geophys. Res. Lett.* **46** 7883
- [183] Qin P, Ge Y, Du A, Huang C, Zhang Y, Luo H, *et al.* 2020 *Astrophys. J. Lett.* **895** L13
- [184] Huang S Y, Fu H S, Yuan Z G, *et al.* 2015 *J. Geophys. Res.* **120** 4496
- [185] Hamrin M, Norqvist P, Karlsson T, Nilsson H, Fu H S, Buchert S, Andre M, Marghito O, Klecker B, Kistler L and Dandouras I 2013 *J. Geophys. Res.* **118** 6279
- [186] Zhou M, Ashour-Abdalla M, Deng X, Schriver D, El-Alaoui M and Pang Y 2009 *Geophys. Res. Lett.* **36** L20107
- [187] Zhou M, Ni B, Huang S, Deng X, Ashour-Abdalla M, Nishimura Y and Yuan Z 2014 *J. Geophys. Res.* **119** 4335
- [188] Deng X, Ashour-Abdalla M, Zhou M, Walker R, El-Alaoui E, Angelopoulos V, Ergun R E and Schriver D 2010 *J. Geophys. Res.* **115** A09225
- [189] Huang S Y, Zhou M, Deng X H, Yuan Z G, Pang Y, Wei Q, Su W, Li H M and Wang Q Q 2012 *Ann. Geophys.* **30** 97
- [190] Fu H S, Cao J B, Cully C M, *et al.* 2014 *J. Geophys. Res.* **119** 9089
- [191] Hwang K J, Goldstein M L, Viñas A F, Schriver D and Ashour-Abdalla M 2014 *J. Geophys. Res.* **119** 2484
- [192] Breuillard H, Le Contel O, Retino A, *et al.* 2016 *Geophys. Res. Lett.* **43** 7279
- [193] Yang J, Cao J B, Fu H S, Wang T Y, Liu W L and Yao Z H 2017 *J. Geophys. Res.* **122** 4299
- [194] Zhang X, Angelopoulos V, Artemyev A V and Liu J 2018 *Geophys. Res. Lett.* **45** 9380
- [195] Chen G, Fu H S, Zhang Y, Su Z P, Liu N G, Chen L, *et al.* 2021 *J. Geophys. Res.* **126** e2020JA028957
- [196] Fu H S, Khotyaintsev Y V, Vaivads A, Retinò A and André M 2013 *Nature Physics* **9** 426
- [197] Fu H S, Grigorenko E E, Gabrielse C, Liu C, Lu S, Hwang K J, Zhou X, Wang Z and Chen F 2020 *Sci. China Earth Sci.* **63** 235
- [198] Fu H S, Zhao M J, Yu Y and Wang Z 2020 *Geophys. Res. Lett.* **47** e2019GL086790
- [199] Zhou M, Deng X H, Ashour-Abdalla M, *et al.* 2013 *J. Geophys. Res.* **118** 674
- [200] Wu M Y, Lu Q M, Volwerk M, *et al.* 2013 *J. Geophys. Res.* **118** 4804
- [201] Wu M Y, Huang C, Lu Q M, Volwerk M, Nakamura R, Vörös Z, Zhang T L and Wang S 2015 *J. Geophys. Res.* **120** 6320
- [202] Tang C L, Lu L, Zhou M and Yao Z H 2013 *Geophys. Res.* **118** 4237
- [203] Huang C, Wu M Y, Lu Q M, Wang R S and Wang S 2015 *J. Geophys. Res.* **120** 1759
- [204] Lu S, Angelopoulos V and Fu H S 2016 *J. Geophys. Res.* **121** 9483
- [205] Lu S, Angelopoulos V, Artemyev A V, Pritchett P L, Liu J, Runov A, *et al.* 2019 *Astrophys. J.* **878** 109
- [206] Grigorenko E E, Kronberg E A, Daly P W, Ganushkina N Y, Lavraud B, Sauvaud J A and Zelenyi L M 2016 *J. Geophys. Res.* **121**
- [207] Liu C M, Fu H S, Xu Y, *et al.* 2017 *J. Geophys. Res.* **122** 594
- [208] Liu C M and Fu H S 2019 *Astrophys. J. Lett.* **873** L2
- [209] Xu Y, Fu H S, Liu C M and Wang T Y 2018 *Astrophys. J.* **853** 11
- [210] Chen G, Fu H S, Zhang Y, Li X, Ge Y S, Du A M, Liu C M and Xu Y 2019 *Astrophys. J. Lett.* **881** L8
- [211] Artemyev A V, Petrukovich A A, Nakamura R and Zelenyi L M 2012 *J. Geophys. Res.* **117** A06219
- [212] Birn J, Hesse M, Nakamura R and Zaharia S 2013 *J. Geophys. Res.* **118** 1960
- [213] Kennel C F and Petschek H E 1966 *J. Geophys. Res.* **71** 1
- [214] Fu H S, Cao J B, Mozer F S, Lu H Y and Yang B 2012 *J. Geophys. Res.* **117** A01203
- [215] Liu C M, Fu H S, Xu Y, Cao J B and Liu W L 2017 *Geophys. Res. Lett.* **44** 6492
- [216] Fu W, Fu H S, Cao J B, Yu Y, Chen Z Z and Xu Y 2022 *J. Geophys. Res.* **127** e2021JA029642
- [217] Runov A, Angelopoulos V, Gabrielse C, Zhou X Z, Turner D and Plaschke F 2013 *J. Geophys. Res.* **118** 744
- [218] Zhao M J, Fu H S, Liu C M, Chen Z Z, Xu Y, Giles B L and Burch J L 2019 *Geophys. Res. Lett.* **46** 2390
- [219] Tang C L, Wang X and Zhou M 2021 *J. Geophys. Res.* **125** e2020JA028787
- [220] Birn J, Thomsen M F and Hesse M 2004 *Phys. Plasmas* **11** 1825
- [221] Birn J, Runov A and Hesse M 2014 *J. Geophys. Res.* **119** 3604
- [222] Huang K, Lu Q M, Huang C, Dong Q L, Wang H Y, Fan F, Sheng Z M, Wang S and Zhang J 2017 *Phys. Plasmas* **24** 102101
- [223] Huang K, Lu Q M, Lu S, Wang R S and Wang S 2021 *J. Geophys. Res.* **126** e2021JA029939
- [224] Thorne R M, Li W, Ni B B, *et al.* 2013 *Nature* **504** 411
- [225] Dai L, Wang C, Duan S P, *et al.* 2015 *Geophys. Res. Lett.* **42** 6170
- [226] Huang S Y, He L H, Yuan Z G, *et al.* 2019 *Astrophys. J.* **875** 113

- [227] Yao S T, Yue Z S, Shi Q Q, Degeling A W, Fu H S, Tian A M, *et al.* 2021 *Earth Planet. Phys.* **5** 63
- [228] Sun W J, Shi Q Q, Fu S Y, *et al.* 2012 *Ann. Geophys.* **30** 583
- [229] Shustov P, Zhang X J, Pritchett P, Artemyev A V, Angelopoulos V, Yushkov E, *et al.* 2019 *J. Geophys. Res.* **124** 342
- [230] Yu Y, Fu H S, Cao J B, Liu Y Y and Wang Z 2022 *Astrophys. J.* **926** 199
- [231] Ge Y S, McFadden J P, Raeder J, Angelopoulos V, Larson D and Constantinescu O D 2011 *J. Geophys. Res.* **116** A01209
- [232] Yao S T, Shi Q Q, Zong Q G, *et al.* 2021 *Astrophys. J.* **923** 216
- [233] Zhima Z, Cao J B, Fu H S, Liu W L, Chen L J, Dunlop M, Zhang X M and Shen X H 2015 *J. Geophys. Res.* **120** 2469
- [234] Yao S T, Shi Q Q, Yao Z H, *et al.* 2019 *Geophys. Res. Lett.* **46** 523
- [235] Liu C M, Fu H S, Liu Y Y and Xu Y 2021 *Geophys. Res. Lett.* **48** e2021GL093174
- [236] Liu Y Y, Fu H S, Olshevsky V, Pontin D I, Liu C M, Wang Z, Chen G, Dai L and Retino A 2019 *Astrophys. J. Suppl.* **244** 31
- [237] Liu Y Y, Fu H S, Zong Q G, Wang Z, Liu C M, Huang S Y, Chen Z Z, Xu Y, Shi Q Q and Yao S T 2020 *Geophys. Res. Lett.* **47** e2020GL088374
- [238] Hutchinson I H 2017 *Phys. Plasmas* **24** 055601
- [239] Lu Q M, Wang D Y and Wang S 2005 *J. Geophys. Res.* **110** A03223
- [240] Lu Q M, Lembege B, Tao J B and Wang S 2008 *J. Geophys. Res.* **113** A11219
- [241] Wu M Y, Lu Q M, Huang C and Wang S 2010 *J. Geophys. Res.* **115** A10245
- [242] Charles C 2007 *Plasma Sources Sci. Technol.* **16** R1
- [243] Wang R S, Lu Q M, Khotyaintsev Y V, *et al.* 2014 *Geophys. Res. Lett.* **41** 4851
- [244] Graham D B, Khotyaintsev Y V, Vaivads A and André M 2015 *Geophys. Res. Lett.* **42** 215
- [245] Norgren C, André M, Vaivads A and Khotyaintsev Y V 2015 *Geophys. Res. Lett.* **42** 1654
- [246] Norgren C, André M, Graham D B, Khotyaintsev Y V and Vaivads A 2015 *Geophys. Res. Lett.* **42** 7264
- [247] Fu H S, Chen F, Chen Z Z, *et al.* 2020 *Phys. Rev. Lett.* **124** 095101
- [248] Moze F S, Agapitov O V, Giles B and Vasko I 2018 *Phys. Rev. Lett.* **121** 135102
- [249] Dai L, Wang C, Cai Z M, *et al.* 2020 *Front. Phys.* **8** 89
- [250] Retino A, Khotyaintsev Y, Le Contel O, *et al.* 2021 *Experimental Astronomy*
- [251] Mozer F S, Bale S D and Phan T D 2002 *Phys. Rev. Lett.* **89** 015002
- [252] Mozer F S, Bale S D, Phan T D and Osborne J A 2003 *Phys. Rev. Lett.* **91** 245002
- [253] Vaivads A, Khotyaintsev Y V, André M, Retino A, Buchert S C, Rogers B N, *et al.* 2004 *Phys. Rev. Lett.* **93** 105001
- [254] Ding D Q, Lee L C and Swift D W 199 *J. Geophys. Res.* **97** 8453
- [255] Swisdak M, Rogers B N, Drake J F and Shay M A 2003 *J. Geophys. Res.* **108** 1218
- [256] Cassak P A and Shay M A 2007 *Phys. Plasmas* **14** 102114
- [257] Pritchett P L 2008 *J. Geophys. Res.* **113** A06210
- [258] Pritchett P L and Mozer F S 2009 *J. Geophys. Res.* **114** A11210
- [259] Pritchett P L and Mozer F S 2009 *Phys. Plasmas* **16** 080702
- [260] Tanaka K G, Retino A, Asano Y, Fujimoto M, Shinohara I, Vaivads A, *et al.* 2008 *Annal. Geophys.* **26** 2471
- [261] Mozer F S, Pritchett P L, Bonnell J B, Sundkvist D and Chang M T 2008 *J. Geophys. Res.* **113** A00C03
- [262] Mozer F S, Angelopoulos V, Bonnell J B, Glassmeier H and McFadden J P 2008 *Geophys. Res. Lett.* **35** L17S04
- [263] Mozer F S, Sundkvist D, McFadden J P, Pritchett P L and Roth I 2011 *J. Geophys. Res.* **116** A12224
- [264] Zhang Y C, Lavraud B, Dai L, *et al.* 2017 *J. Geophys. Res.* **122** 5277
- [265] Hesse M, Aunai N, Sibeck D and Birn J 2014 *Geophys. Res. Lett.* **41** 8673
- [266] Hesse M, Liu Y H, Chen L J, Bessho N, Kuznetsova M, Birn J and Burch J L 2016 *Geophys. Res. Lett.* **43** 2359
- [267] Shay M A, Phan T D, Haggerty C C, Fujimoto M, Drake J F, Malakit K, *et al.* 2016 *Geophys. Res. Lett.* **43** 4145
- [268] Swisdak M, Drake J F, Price L, Burch J L, Cassak P A and Phan T D 2018 *Geophys. Res. Lett.* **45** 5260
- [269] Sang L L, Lu Q M, Wang R S, Huang K and Wang S 2018 *Phys. Plasmas* **25** 062120
- [270] Sang L L, Lu Q M, Wang R S, Huang K and Wang S 2019 *Astrophysical Journal* **877** 155
- [271] Sang L L, Lu Q M, Wang R S, Huang K and Wang S 2019 *Astrophysical Journal* **882** 126
- [272] Wang S, Chen L J, Bessho N, Hesse M, Yoo J, Yamada M, *et al.* 2018 *J. Geophys. Res.* **123** 8185
- [273] Chang C, Huang K, Lu Q M, Sang L L, Lu S, Wang R S, *et al.* 2021 *J. Geophys. Res.* **126** e2021JA029290
- [274] Burch J L, Torbert R B, Phan T D, Chen L J, Moore T E, Ergun R E, *et al.* 2016 *Science* **352** aaf2939
- [275] Phan T D, Eastwood J P, Cassak P A, Oieroset M, Gosling J T, Gershman D J, *et al.* 2016 *Geophys. Res. Lett.* **43** 6060
- [276] Fu H S, Cao J B, Cao D, Wang Z, Vaivads A, Khotyaintsev Y V, *et al.* 2019 *Geophys. Res. Lett.* **46** 48
- [277] Fu H S, Peng F Z, Liu C M, Burch J L, Gershman D G and Le Contel O 2019 *Geophys. Res. Lett.* **46** 5645
- [278] Wang Z, Fu H S, Liu C M, Liu Y Y, Cozzani G, Giles B L, *et al.* 2019 *Geophys. Res. Lett.* **46** 1195
- [279] Wang Z, Fu H S, Vaivads A, Burch J L, Yu Y and Cao J B 2020 *Astrophysical Journal Letters* **899** L34
- [280] Peng F Z, Fu H S, Cao J B, Graham D B, Chen Z Z, Cao D, *et al.* 2017 *J. Geophys. Res.* **122** 6349
- [281] Chen Y X, Toth G, Cassak P, Jia X Z, Gombosi T I, Slavin J A, *et al.* 2017 *J. Geophys. Res.* **122** 10318
- [282] Chen Y X, Toth G, Hietala H, Vines S K, Zou Y, Nishimura Y, *et al.* 2020 *Earth and Space Science* **7** e2020EA001331
- [283] Khotyaintsev Y V, Graham D B, Norgren C, Eriksson E, Li W, Johlander A, *et al.* 2016 *Geophys. Res. Lett.* **43** 5571
- [284] Lavraud B, Zhang Y C, Vernisse Y, Gershman D J, Dorelli J, Cassak P A, *et al.* 2016 *Geophys. Res. Lett.* **43** 3042
- [285] Zhou M, Berchem J, Walker R J, El-Alaoui M, Deng X, Cazzola E, *et al.* 2017 *Phys. Rev. Lett.* **119** 055101
- [286] Eastwood J P, Goldman M V, Phan T D, Stawarz J E, Cassak P A, Drake J F, *et al.* 2020 *Phys. Rev. Lett.* **125** 265102
- [287] Tang B B, Li W Y, Le A, *et al.* 2020 *Geophys. Res. Lett.* **47** e2020GL087159
- [288] Zhou M, Ashour-Abdalla M, Berchem J, Walker R J, Liang H, El-Alaoui M, *et al.* 2016 *Geophys. Res. Lett.* **43** 4808
- [289] Wilder F D, Ergun R E, Goodrich K A, Goldman M V, Newman D L, Malaspina D M, *et al.* 2016 *Geophys. Res. Lett.* **43** 5909
- [290] Cao D, Fu H S, Cao J B, Wang T Y, Graham D B, Chen Z Z, *et al.* 2017 *Geophys. Res. Lett.* **44** 3954
- [291] Ergun R E, Chen L J, Wilder F D, Ahmadi N, Eriksson S, Usanova M E, *et al.* 2017 *Geophys. Res. Lett.* **44** 2978
- [292] Li W, Li J X, Li W T, *et al.* 2020 *Nat. Commun.* **11** 141
- [293] Ren Y, Dai L, Wang C, Li W, Tao X, Lavraud B and Le Contel O 2021 *Geophys. Res. Lett.* **48** e2020GL090816
- [294] Dungey J W 1961 *Phys. Rev. Lett.* **6** 47
- [295] Russell C T and Elphic R C 1978 *Space Sci. Rev.* **22** 681
- [296] Lee L C and Fu Z F 1985 *Geophys. Res. Lett.* **12** 105
- [297] Scholer M 1988 *Geophys. Res. Lett.* **15** 748
- [298] Hasegawa H, Sonnerup B U O, Owen C J, Klecker B, Paschmann G, Balogh A and Reme H 2006 *Annal. Geophys.* **24** 603
- [299] Hasegawa H, Wang J, Dunlop M W, Pu Z Y, Zhang Q H, Lavraud B, *et al.* 2010 *Geophys. Res. Lett.* **37** L16101
- [300] Oieroset M, Phan T D, Eastwood J P, Fujimoto M, Daughton W, Shay M A, *et al.* 2011 *Phys. Rev. Lett.* **107** 165007
- [301] Zhong J, Pu Z Y, Dunlop M W, Bogdanova Y V, Wang X G, Xiao C J, *et al.* 2013 *J. Geophys. Res.* **118** 1904
- [302] Raeder J 2006 *Annal. Geophys.* **24** 381
- [303] Dorelli J C and Bhattacharjee A 2009 *J. Geophys. Res.* **114** A06213
- [304] Gloer A, Dorelli J, Toth G, Komar C M and Cassak P A 2016 *J. Geophys. Res.* **121** 140
- [305] Sun T R, Tang B B, Wang C, Guo X C and Wang Y 2019 *J. Geophys. Res.* **124** 2425
- [306] Chen C, Sun T R, Wang C, Huang Z H, Tang B B and Guo X C 2019 *Geophys. Res. Lett.* **46** 4106
- [307] Winglee R M, Harnett E, Stickle A and Porter J 2008 *J. Geophys. Res.* **113** A02209
- [308] Omid N and Sibeck D G 2007 *Geophys. Res. Lett.* **34** L04106
- [309] Sibeck D G and Omid N 2012 *Journal of Atmospheric and Solar-Terrestrial Physics* **87–88** 20

- [310] Hoilijoki S, Ganse U, Pfau-Kempf Y, Cassak P A, Walsh B M, Hietala H, *et al.* 2017 *J. Geophys. Res.* **122** 2877
- [311] Hoilijoki S, Ganse U, Sibeck D G, Cassak P A, Turc L, Battarbee M, *et al.* 2019 *J. Geophys. Res.* **124** 4037
- [312] Tan B, Lin Y, Perez J D and Wang X Y 2011 *J. Geophys. Res.* **116** A02206
- [313] Tan B, Lin Y, Perez J D and Wang X Y 2012 *J. Geophys. Res.* **117** A03217
- [314] Guo J, Lu S, Lu Q M, Lin Y, Wang X Y, Huang K, *et al.* 2021 *J. Geophys. Res.* **126** e2021JA029388
- [315] Guo J, Lu S, Lu Q M, Lin Y, Wang X Y, Huang K, *et al.* 2021 *J. Geophys. Res.* **126** e2020JA028670
- [316] Dungey J W 1963 "The structure of the ionosphere, or adventures in velocity space". Edited by DeWitt C, Hiebolt J and Lebeau A, *Geophysics: The Earth's Environment* (New York: Gordon and Breach) pp. 526–536
- [317] Gosling J T, Thomsen M F, Bame S J, Elphic R C and Russell C T 1991 *J. Geophys. Res.* **96** 14097
- [318] Lavraud B, Thomsen M F, Lefebvre B, Schwartz S J, Seki K, Phan T D, *et al.* 2006 *J. Geophys. Res.* **111** A05211
- [319] Shi Q Q, Zong Q G, Fu S Y, Dunlop M W, Pu Z Y, Parks G K, *et al.* 2013 *Nat. Commun.* **4** 1466
- [320] Frey H U, Phan T D, Fuselier S A and Mende S B 2003 *Nature* **426** 533
- [321] Phan T, Frey H U, Frey S, Peticolas L, Fuselier S, Carlson C, *et al.* 2003 *Geophys. Res. Lett.* **30** 1509
- [322] Lockwood M and Moen J 1999 *Annal. Geophys.* **17** 996
- [323] Zhang H, Zong Q G, Fritz T A, Fu S Y, Schaefer S, Glassmeier K H, *et al.* 2008 *J. Geophys. Res.* **113** A03204
- [324] Zhang Q H, Moen J, Lockwood M, McCreia I, Zhang B C, McWilliams K A, *et al.* 2016 *J. Geophys. Res.* **121** 9063
- [325] Fuselier S A, Petrincec S M, Trattner K J and Lavraud B 2014 *J. Geophys. Res.* **119** 9051
- [326] Zong Q G, Fritz T A, Spence H, *et al.* 2005 *Geophys. Res. Lett.* **32** L01101
- [327] Hasegawa H, Retino A, Vaivads A, Khotyaintsev Yu, Nakamura R, Takada T, *et al.* 2008 *Geophys. Res. Lett.* **35** L15104
- [328] Berchem J, Raeder J and Ashourabdalla M 1995 *Geophys. Res. Lett.* **22** 1189
- [329] Grandin M, Turc L, Battarbee M, Ganse U, Johlander A, Pfau-Kempf Y, *et al.* 2020 *Journal of Space Weather and Space Climate* **10** 51
- [330] Guo J, Lu S, Lu Q M, Lin Y, Wang X Y, Zhang Q H, *et al.* 2021 *Geophys. Res. Lett.* **48** e2021GL095003
- [331] Tsurutani B T and Stone R G 1985 *Collisionless shocks in the heliosphere: Reviews of current Research* (Washington, D C: American Geophysical Union)
- [332] Leory M M, Winske D, Goodrich C C, Wu C S and Papadopoulos K 1982 *J. Geophys. Res.* **87** 5081
- [333] Lembège B, Savoini P, Hellinger P and Travnicek P M 2009 *J. Geophys. Res.* **114** A03217
- [334] Yang Z W, Lu Q M, Lembege B and Wang S 2009 *J. Geophys. Res.* **114** A03111
- [335] Burgess D 1989 *Geophys. Res. Lett.* **16** 345
- [336] Winske D, Omid N, Quest K B and Thomas V A 1990 *J. Geophys. Res.* **95** 18821
- [337] Scholer M and Burgess D 1992 *J. Geophys. Res.* **97** 8319
- [338] Wu M Y, Hao Y F, Lu Q M, Huang C, Guo F and Wang S 2015 *Astrophys. J.* **808** 2
- [339] Schwartz S J, Burgess D, Wilkinson W P, Kessel R L, Dunlop M and Lühr H 1992 *J. Geophys. Res.* **97** 4209
- [340] Su Y Q, Lu Q M, Huang C, Wu M Y, Gao X L and Wang S 2012 *J. Geophys. Res.* **117** A08107
- [341] Wilson L B III, Koval A, Sibeck D G, Szabo A, Cattell C A, Kasper J C, Maruca B A, Pulupa M, Salem C S and Wilber M 2013 *J. Geophys. Res.* **118** 957
- [342] Hao Y F, Lu Q M, Gao X L and Wang S 2016 *Astrophys. J.* **823** 7
- [343] Yordanova E, Vörös Z, Varsani A, Graham D B, Norgren C, Khotyaintsev Y V, *et al.* 2016 *Geophys. Res. Lett.* **43** 5969
- [344] Gingell I, Schwartz S J, Burgess D, Johlander A, Russell C T, Burch J L, *et al.* 2017 *J. Geophys. Res.* **122** 11003
- [345] Phan T D, Eastwood J P, Shay M A, Drake J F, Sonnerup B U Ö, Fujimoto M, *et al.* 2018 *Nature* **557** 202
- [346] Guo Z, Lin Y, Wang X Y and Du A M 2018 *J. Geophys. Res.* **123** 9169
- [347] Lu Q M, Wang H Y, Wang X Y, Lu S, Wang R S, Gao X L and Wang S 2020 *Geophys. Res. Lett.* **47** e2019GL085661
- [348] Wang S M, Wang R S, Lu Q M, Russell C T, Ergun R E and Wang S 2021 *Geophys. Res. Lett.* **48** e2021GL094879
- [349] Pyakurel P S, Shay M A, Phan T D, *et al.* 2019 *Phys. Plasmas* **26** 082307
- [350] Wang S, Chen L J, Bessho N, Hesse M, Wilson L B III, Giles B, *et al.* 2019 *Geophys. Res. Lett.* **46** 562
- [351] Lu Q M, Yang Z W, Wang H Y, Wang R S, Huang K, Lu S and Wang S 2021 *Astrophys. J.* **919** 28
- [352] SMILE science study team 2018 *SMILE (Solar Wind Magnetosphere Ionosphere Link Explorer) Definition Study Report*, ESA/SCI(2018) 1, December, 2018